



# Freeze Casting with Bioceramics for Bone Graft Substitutes

Tony J. Yin<sup>1</sup> · Steven E. Naleway<sup>1</sup>

Received: 23 June 2022 / Accepted: 2 August 2022  
© The Author(s), under exclusive licence to Springer Science+Business Media, LLC 2022

## Abstract

Freeze casting with bioceramics affords the opportunity to create the next generation of bone graft substitutes. Because of its versatile material fabrication process and effective methods of structural control, freeze casting helps to meet the many criteria that are required of viable bone graft substitute biomaterials. In combination with biocompatible and resorbable ceramics and ceramic composites that can offer bone growth through osteoconduction, this process helps provide a tailored pore structure while maintaining the necessary mechanical properties for bone growth. Here, the advantages of freeze casting with bioceramics for orthopedic and dental applications are summarized: in particular, these advantages include its compatibility with a large variety of bioceramics, many forms of both uniform and localized structure control, and its ability to be used in combination with other advanced manufacturing processes.

**Keywords** Freeze casting · Bioceramics · Bone graft substitutes · Property control · Material fabrication

## Introduction

Freeze casting to fabricate bone graft substitutes has garnered great interest in the past two decades. This technique for the construction of porous structures has many benefits to meet the requirements of *biomaterials*, materials engineered to work in tandem with biological systems. When combined with ceramic biomaterials, referred to herein as *bioceramics*, freeze casting could lead to the next generation of bone graft substitutes.

In this review, we have detailed how freeze casting has the potential to satisfy the many requirements of biomaterials, thus making it an excellent technique for fabricating bone graft substitutes. In particular, here we will focus on: (1) the variety of bioceramics and their composites used with freeze casting for the purpose of creating bone graft substitutes and (2) the different methods that researchers have used to control and tailor their porous freeze-cast structures while using these bioceramics. Along with its compatible usage with all types of materials and its various controls to generate a tailored pore structure, freeze casting offers possibilities in

composite fabrication and unique structures when combined with other advanced manufacturing processes.

Summaries of freeze casting with biomaterials provided by Deville et al. [1] and Wegst et al. [2] have focused on the physics and principles involved in the freeze-casting process and offer insights into how the process can differ through alterations to the initial conditions. Nelson and Naleway [3] have described intrinsic and extrinsic control methods that can be used during the freezing process. Bioinspired freeze-cast structures and new applications and materials for freeze casting have been reviewed recently, with foci on broader applications such as energy storage or structural applications [4, 5]. A review on freeze casting with biopolymers for biological tissue engineering has also been discussed by Qin et al. [6]. In deference of these topics, this review instead emphasizes how the specific advantages of freeze casting through material use and structural control can be implemented to create bioceramics for orthopedic and dental applications.

## Biomaterial Requirements

Bone grafts and bone graft substitutes accounted for the largest share of the biosurgery global market in 2020, with increased usage in orthopedic and dental surgeries [7]. An estimated 2.2 million orthopedic bone graft procedures are performed each year, with 500,000 estimated to occur

✉ Steven E. Naleway  
steven.naleway@mech.utah.edu

<sup>1</sup> Department of Mechanical Engineering, University of Utah, Salt Lake City, USA

in the United States, a trend that is likely to increase as the geriatric population increases [8–11]. Additionally, cosmetic improvements such as oral and cranio-/maxillo-facial surgeries are on the rise, with another estimated 500,000 cosmetic dental implant procedures occurring in the US in 2019 [12]. Sports injuries and bone deformities in pediatric patients have also led to increased usage of orthopedic and dental implants [13, 14]. With the expected global increase in procedures, there persists a demand for the development of better, marketable bone graft substitutes [7, 11, 12, 14].

With the main goal to regrow and provide support to the surrounding bone tissue, multiple interconnected criteria define a viable bone graft substitute biomaterial based on both the material composition and structural properties of the scaffold [15–17]:

1. The biomaterial must be biocompatible (Fig. 1a), meaning it will provide an environment that meets the nutritional and biological needs for bone cells to grow [18]. The biomaterial should also aim to limit cytotoxicity, immunogenicity, or other negative responses (Fig. 1b) as dictated by standards such as ISO 10993-1, Biological Evaluation of Medical Devices [19].
2. The biomaterial should promote bone growth and biological performance through osteoconduction, osteoinduction, and osteogenesis (Fig. 1c). Osteoconduction is the ability to spread osteoblasts cells along a surface through cell adhesion, proliferation, and migration [20]. Osteoinduction, or the signaling of osteogenesis typically through growth factors, is the ability to signal, recruit, and differentiate stem cells and osteoblasts through bone healing protocols at a repair site [21–23]. Osteogenic biomaterials should contain the cells, growth factors, and the appropriate pore structure required to grow new bone [24].
3. The biomaterial must have appropriate mechanical strength that matches that of the implant location, properly distributing the load to the surrounding bone (Fig. 1d). The exact required properties need to vary with the targeted application. Mismatched mechanical properties (Fig. 1e) can lead to implant loosening, failure, and fracture [8, 25, 26]. Trabecular or cancellous bone has a measured ultimate compressive strength of 2–20 MPa and an elastic modulus ranging from 0.1 to 5 MPa [27]. Cortical or compact bone has greater strength at 100–230 MPa [28] and elastic modulus from 7 to 30 GPa [29]. Additional mechanical properties that should be considered include hardness and fatigue life [28]. Bone also exhibits orthotropic structural and mechanical properties, so matching the mechanical properties relies on both the material composition and pore structure [10].
4. The biomaterial must have adequate porosity to allow for vascularization, cell proliferation and migration, nutrient transportation, and waste removal (Fig. 1f, g) [8, 10, 30]. Bone is naturally a porous material, so a viable biomaterial should mimic that. Unfortunately, a porous structure negatively affects mechanical strength, leading to the need to compromise between porosity and strength [1, 31]. Studies on bone substitutes have found the ideal pore size should be greater than 100  $\mu\text{m}$  to allow for new bone formation, with smaller pores leading to less observed bone growth [32]. Pores greater than 300  $\mu\text{m}$  were reported to produce the most vascularization and new bone formation [15]. A total porosity of at least 60% and the addition of microporosity in structural walls have also been reported to improve bone growth [33–35].
5. The biomaterial must have a controllable resorption rate [36–39] and safe biodegradability (Fig. 1h) [40]. Resorption is a step in the process of bone remodeling where the mineral phase is broken down and returned to the body. In the human body, all of the bone is resorbed and remodeled within a period of about six-to-seven months [41]. Given this time constraint, a biomaterial that degrades too quickly will outpace the bone's remodeling, leaving a weakened pore structure. In addition, biodegradable products must not create toxic byproducts lest they harm the body [15]. In the event of a bioinert material that cannot be degraded (Fig. 1i), any particulates that accumulate from frictional wear must be non-cytotoxic both locally and systemically [42].

With so many requirements, many biomaterials tend to meet only a couple of the requirements instead of all of them (e.g., metal hip stems that provide high mechanical strength, but never resorb and are not osteogenic [43]), thus resulting in suboptimal products and negative patient outcomes like secondary surgeries [30, 44] and material failures [10, 45].

As shown in Table 1, current solutions for bone graft substitute biomaterials are as follows: (1) autografts, which are harvested from other areas of the patient's own body; (2) allografts, which are sourced and processed from human donors; (3) xenografts, which are sourced from donors of other species (e.g., from bovine bone); and (4) alloplasts (e.g., as is the focus of this review, ceramic alloplasts or bioceramics), which are artificially synthesized. Autografts remain the gold standard for bone graft substitutes for their biological safety with little risk of immunogenicity, and they naturally possess the cells and the vascularized pore structure required for osteoconduction, osteoinduction, and osteogenesis [10]. However, complications can arise from the multiple necessary surgeries leading to pain and higher costs [15, 46]. Consequently, autografts are limited to smaller bone defects. Allografts sourced from human donors, living

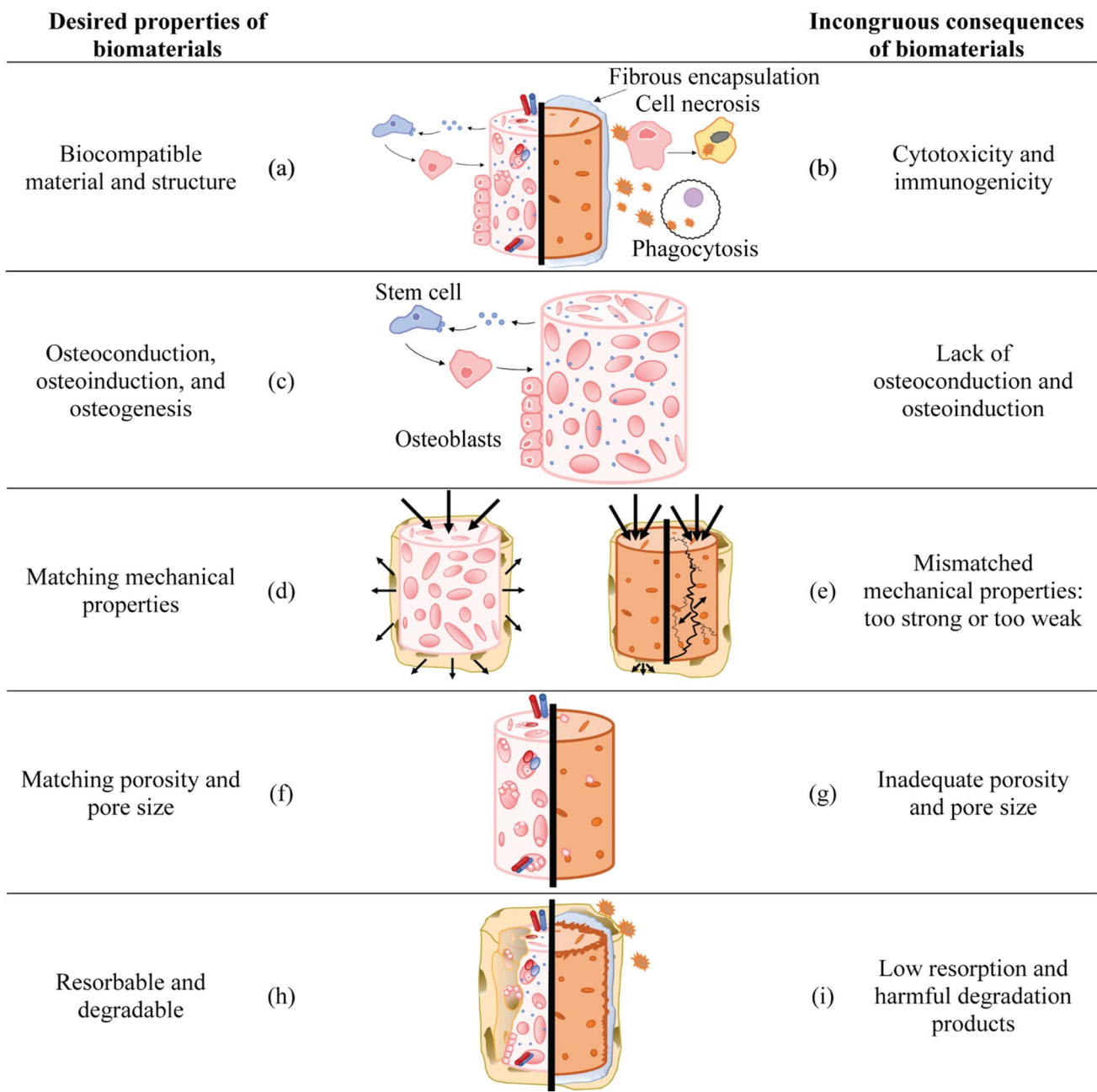


**Fig. 1** Illustrated requirements of biomaterials. **a** (left half, pink) An implant with biocompatible material and structure that allows for proper bone growth and provides an environment to support bone healing. **b** (right half, orange) A hazardous implant that is cytotoxic and immunogenic causing cell necrosis, phagocytosis of implant particulates, and fibrous encapsulation. **c** An osteoconductive and osteoinductive biomaterial that allows for proliferation and migration of osteoblast cells as well as the recruitment of stem cells for osteogenesis. **d** (left, pink) A biomaterial with matching mechanical properties that distributes the load to surrounding bone. **e** Biomaterials with mismatched mechanical properties, (left half, orange) a material that

is too strong or stiff and does not transfer enough load to surrounding bone, (right half, orange) a material that is too weak and experiences cracking and implant failure under loading. **f** (left half, pink) A biomaterial with matching porosity and pore size leading to cell migration into the pores and angiogenesis. **g** (right half, orange) Inadequate porosity and pore size leading to limited cell growth. **h** (left half, pink) A resorbable and biodegradable biomaterial leading to eventual replacement from bone growth. **i** (right half, orange) A biomaterial with low resorption and potentially harmful degradation products ultimately leading to fibrous encapsulation

**Table 1** Types of commonly used bone graft substitutes

Type	Material source	Advantages	Disadvantages
Autografts	Patient: Extraoral/intraoral bone	<ul style="list-style-type: none"> <li>•Osteoconductive</li> <li>•Osteoinductive</li> <li>•Osteogenesis</li> <li>•Matching structural strength</li> <li>•Matching resorption</li> <li>•No immunogenicity</li> </ul>	<ul style="list-style-type: none"> <li>•Reliance on patient tissue quality and availability</li> <li>•Pain</li> <li>•Infection</li> </ul>
Allografts	Human donors: Freeze-dried bone allografts Demineralized bone matrix	<ul style="list-style-type: none"> <li>•Cadaveric sourcing</li> <li>•No harvest surgery</li> <li>•Osteoconductive</li> <li>•Matching structural strength</li> <li>•Matching resorption</li> </ul>	<ul style="list-style-type: none"> <li>•Necessary sterilization</li> <li>•Limited osteoinduction</li> <li>•Reduced properties from sterilization</li> <li>•Low risk of disease transmission</li> <li>•Patient ethical/religious concerns of source</li> </ul>
Xenografts	Animal donors: porcine/bovine/coral	<ul style="list-style-type: none"> <li>•Economical sourcing</li> <li>•No harvest surgery</li> <li>•Osteoconductive</li> <li>•Matching resorption</li> </ul>	<ul style="list-style-type: none"> <li>•Necessary sterilization</li> <li>•No osteoinduction</li> <li>•Reduced properties from sterilization</li> <li>•Low risk of disease transmission</li> <li>•Patient ethical/religious concerns of source</li> </ul>
Ceramic alloplasts	Artificial constructs: HA, $\beta$ -TCP, BG, $\text{Al}_2\text{O}_3$ , $\text{TiO}_2$ , $\text{ZrO}_2$ , etc.	<ul style="list-style-type: none"> <li>•Synthetic sourcing</li> <li>•No harvest surgery</li> <li>•Osteoconductive</li> <li>•Tailorable structures and materials</li> <li>•Similarity to bone mineral</li> <li>•Resorbable</li> <li>•No disease transmission</li> </ul>	<ul style="list-style-type: none"> <li>•Necessary sterilization</li> <li>•Limited osteoinduction</li> <li>•Needs optimization to match bone properties</li> <li>•Brittle</li> <li>•Difficulty controlling resorption</li> </ul>

or deceased, are the primary alternative to autografts [10, 15]. However, these materials require sterilization to prevent potential disease transmission, which can reduce the effectiveness of the material in terms of mechanical strength and osteoinduction [47]. Similarly, xenografts obtained from porcine [48], bovine [49], coral [50], and other [51] nonhuman sources also require sterilization to prevent potential interspecies disease transmission like bovine spongiform encephalopathy or porcine endogenous retroviruses.

In addition to the market prospects and biomaterial requirements, patient concerns with the source of the product material should also be considered [52, 53]. Patient survey studies on the preferences of bone graft materials found the highest refusal rates for allografts, extraoral autografts, and xenografts [54, 55]. Some of the reasons for refusal include religious and ethical motivations for allografts and xenografts, and fear of pain for autografts [54]. On the other hand, alloplasts showed the lowest refusal rates along with intraoral autografts [54, 55]. Therefore, there exists the need for products that can achieve the desired bone growth properties while also meeting clinical demands, leading to a plethora of research into suitable alloplastic biomaterials.

Promising research on synthetic alloplasts has produced many constructs from the different classes of materials: metals, ceramics, polymers, and composites [15, 24, 46]. The appeal of these biomaterials lies in their multitudinous manufacturing processes, limitless combinations, and adaptability toward the desired applications. Because these materials

are synthetically made, they have an edge over autografts which require extra surgeries and also over allografts and xenografts which have a small risk of disease transmission. With these advantages, alloplasts with hierarchical porous structures, biocompatible and resorbable materials, and tailored mechanical properties mimicking bone can be fabricated. However, despite their great potential as bone graft substitutes, each group of materials faces hurdles that must be overcome: metals often remain inert and can introduce cytotoxic particulate from wear or implant loosening because they are much stronger than bone, ceramics remain brittle which limits their use in load-bearing regions and can lead to catastrophic failure, polymers degrade rapidly and lack mechanical strength, and composites often require complex, expensive manufacturing processes [15, 24, 42, 46]. Additionally, many materials lack osteoinductive capabilities, thus, further research into osteoinduction through growth factors or other methods is necessary to match the osteogenic potential of autografts. Furthermore, matching the anisotropic structure and mechanical properties of bone still remains a challenge [15, 24, 42, 46].

### Freeze-Casting Principle

Several methods have been used to fabricate porous biomaterials for bone graft substitutes. Examples include polymer replication [56, 57], solid freeform fabrication [58], and rapid prototyping [59, 60], to name a few. These methods

typically provide an isotropic microstructure. To produce anisotropy closer to that of natural bone, alternative methods should be employed. One particularly promising technique is freeze casting [1, 61].

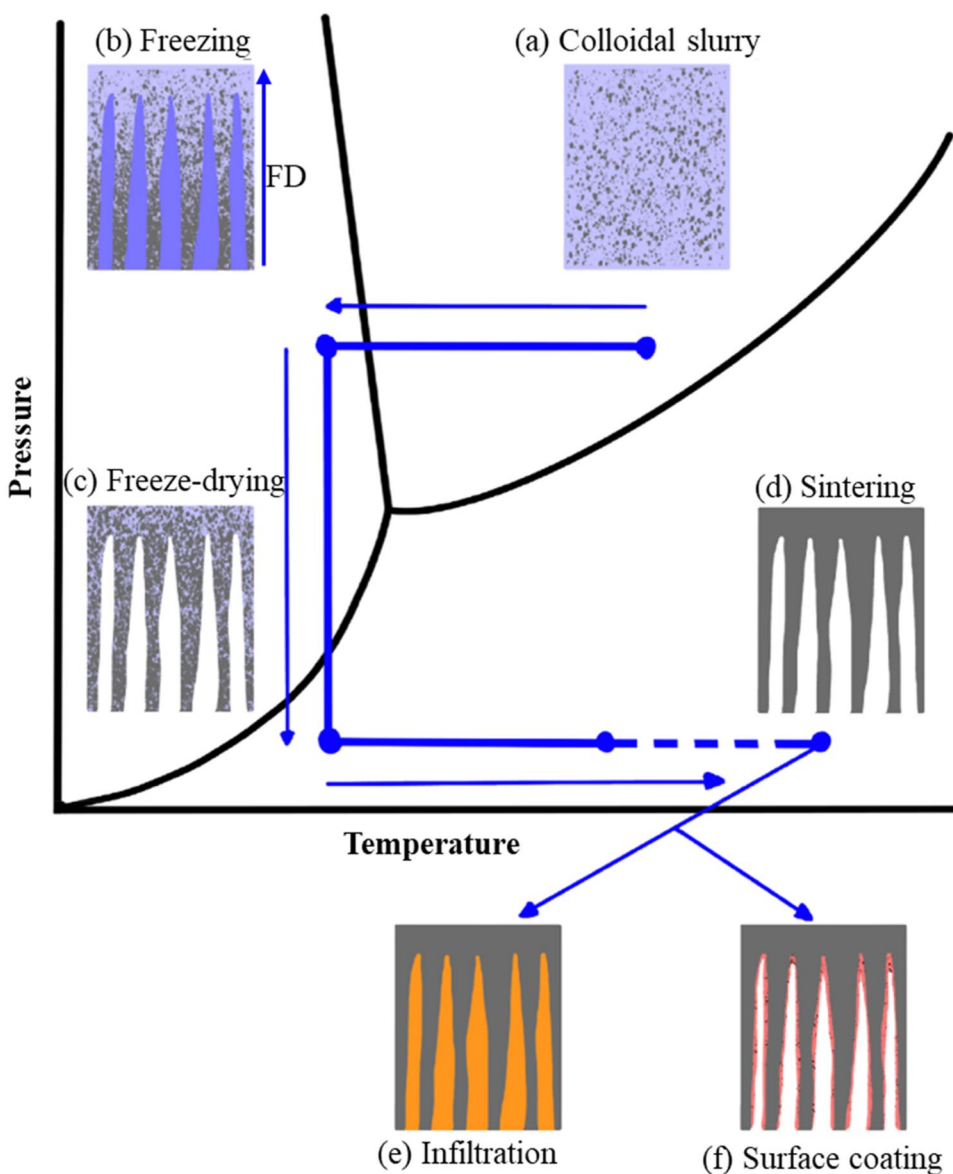
Freeze casting offers many advantages for manufacturing biomaterials because of its relatively simple physical process that remains mostly independent of the solid material [1, 5]. While freeze casting has been achieved with a variety of solid materials (e.g., polymers, metals, and composites), it has primarily been used with ceramics [1, 2, 61, 62]. As such, the discussion herein will concentrate on freeze casting with bioceramics, specifically focused on endeavors to create bone graft substitutes mimicking natural bone.

Ceramic freeze casting involves four main steps (Fig. 2a–d):

1. Mixing of a solvent with ceramic particles to form a colloidal slurry,
2. The freezing of the colloidal slurry at a controlled rate,
3. Sublimation of the solvent under low temperature and pressure to form a green body, and
4. Sintering of the green body to consolidate the structure and increase mechanical strength.

Unidirectional freeze casting using a single freezing direction is the most common form of freeze casting. The freeze-casting process results in a porous scaffold where the pore structure is the negative of the frozen solvent. Additional post-processing can be performed with examples including infiltrating (Fig. 2e) or surface coating (Fig. 2f) the porous scaffold with another material to

**Fig. 2:** 4-step unidirectional freeze-casting process shown on a pressure–temperature diagram. **a** Mixing of a colloidal slurry. **b** Freezing of the slurry with a vertical freezing direction (FD). **c** Freeze drying, sublimation, at low temperature and pressure to remove the solvent. **d** Sintering at high temperature to densify structure. **e** Post-processing through infiltration of structure. **f** Post-processing through coating of the pore surfaces



produce a composite or altering the surface properties of the scaffold to better match the surface of bone.

To elaborate on the nuances of the process, the initial colloidal slurry requires proper dispersion of the ceramic particles. If sedimentation occurs, no porosity will appear, therefore, a dispersant is added to maintain colloidal homogeneity. As the solvent freezes, often through contact with a freezing element or cold finger, the ceramic particles are pushed aside by the solidifying solvent [2, 61, 62]. This freezing front traps the ceramic particles between the solvent crystals. If the freezing process occurs too quickly, then the ceramic particles will be absorbed into the freezing front, producing a homogenous, monolithic structure [63]. To maintain structural stability during sublimation, polymeric binders are added to the initial colloidal slurry. These binders are generally removed during sintering through pyrolysis [3, 61].

The properties of freeze-cast scaffolds can be controlled through various parameters during the freezing process. These parameters are often used to control the pore structure and properties, but can also affect the mechanical properties [3], as demonstrated when comparing the inverse relationship between porosity and mechanical strength [1]. These parameters can generally be categorized into intrinsic and extrinsic control methods [3]. Intrinsic controls, which are defined as those that act within the freezing process [3], include changes to the particle quantity and size [64–66], changes to the particle shape [5, 67–69], solvent choice [70], the presence and types of additives [71–73], and changes to the freezing rate [74, 75]. Intrinsic control methods can affect the global microstructure and porosity but tend to act uniformly, thus lacking the influence to enact localized alterations in the pore structure. Extrinsic controls, which are defined as those that act upon the freezing process through external influences [3], include the use of sacrificial templates [76–78], changes in the freezing direction [79], multi-step freezing [80], and the use of applied energized fields such as magnetic [67, 81, 82], electric [83–85], and ultrasonic fields [86–88]. Extrinsic control methods allow for more complex pore structures to be made, with hierarchical and localized anisotropy that can differ across multiple length scales and locations.

Tanaka et al. [34] offers a great example of the benefits that freeze casting offers for creating bone graft substitutes. In this work, they evaluated the properties of scaffolds that had aligned pores through freeze casting or randomly oriented, interconnected pores through another method. The freeze-cast scaffolds allowed for better *in vitro* cell proliferation in the scaffold interior. They continued their study *in vivo* using mice and observed greater bone regeneration within the freeze-cast scaffold compared to the scaffold with randomly oriented, interconnected pores. These improvements were deduced as the results of the anisotropic

structure obtained through freeze casting. The aligned pores allowed for a higher compressive strength and porosity in the applied directions, improving cell proliferation and load distribution. Additionally, capillary action was observed during cell seeding, providing an easier pathway for cells to travel when compared to the tortuous pores in the interconnected structure.

To meet the need for suitable bone graft substitutes, freeze casting with bioceramics can be used to create porous, mechanically sound biomaterials with appropriate biocompatibility, bone growth, and timely resorption. Freeze casting consists of a straightforward, physical process that is compatible with all types of materials and offers versatile control methods. The technique also offers the means to create tailored, anisotropic pore structures with matching mechanical strength to promote bone ingrowth and vascularization. In summation, our aim is to emphasize two advantages that freeze casting with bioceramics offers for fabricating bone graft substitutes: (1) freeze-cast biomaterials can be fabricated with numerous types bioceramics and their composites, and (2) freeze casting with bioceramics offers many control methods to create both uniform and localized tailored pore structures as necessitated for orthopedic and dental applications.

## Freeze Casting with Bioceramics

While freeze casting can be performed with many materials, a large number of these materials are inappropriate as bone biomaterials or do not fit within the definition of bioceramics. To define what consists of a bioceramic, the authors have decided to consider any material that consists of at least 50% ceramic by composition, excluding those ceramics not generally accepted as viable for biological applications. Here, we will discuss the most commonly applied bioceramics that have been used with freeze casting for bone graft substitute applications with examples of such materials shown in Fig. 3.

### Calcium Phosphates

As a calcium phosphate (CP), hydroxyapatite (HA)  $[\text{Ca}_{10}(\text{PO}_4)_6(\text{OH})_2]$  (Fig. 3a) is one of the most commonly used materials for bone substitutes because of its similar chemical composition to the mineral phase in bone [89]. HA shows exceptional osteoconductivity [90] with potential for osteoinductivity [91–93] as well and low solubility when compared to other calcium phosphates [94, 95]. This low solubility leads to slower resorption rates, with HA implants only showing full replacement with natural bone after more than five years [96, 97]. Many reports detail the properties of freeze-cast HA scaffolds. Reported solid

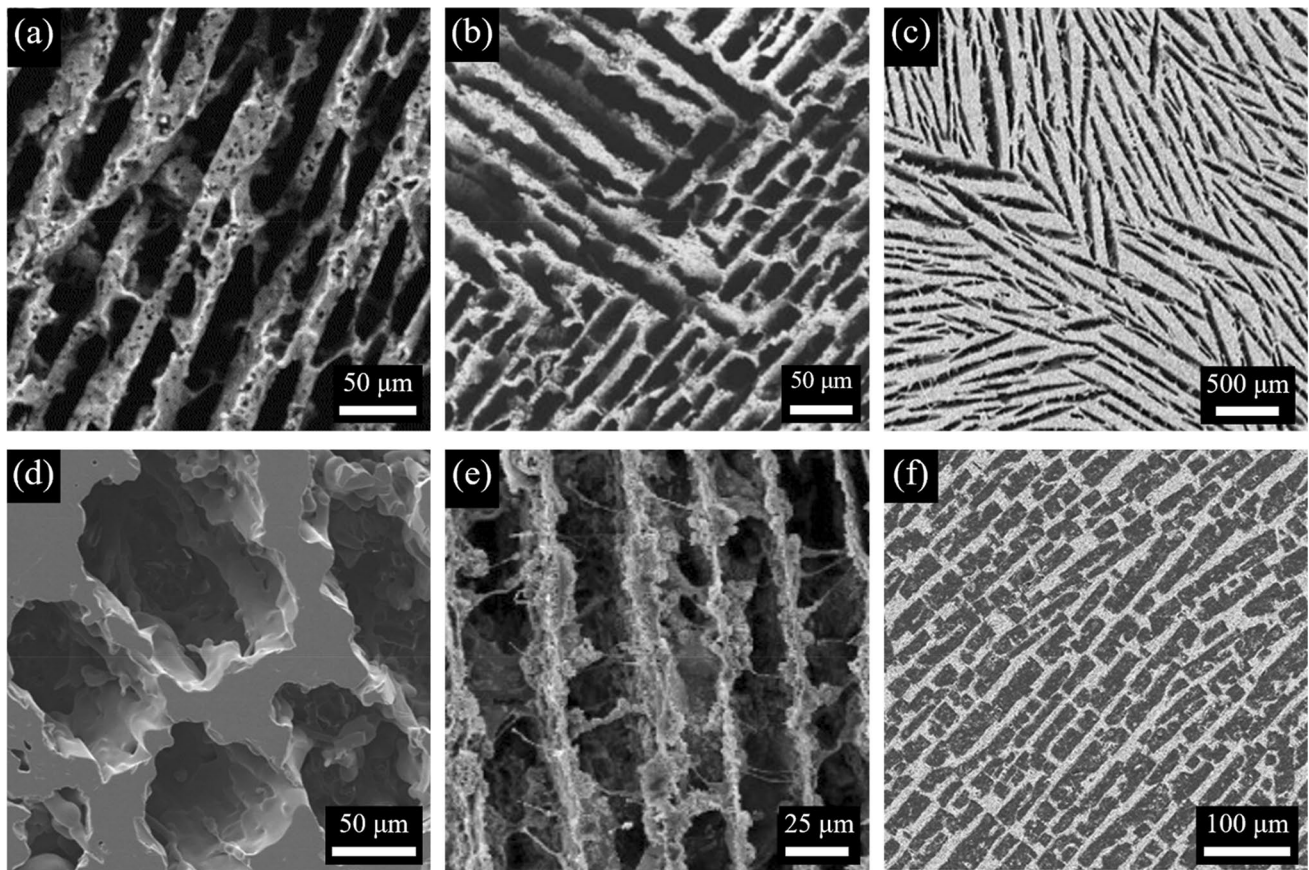


**Fig. 3** Scanning electron microscopy images for freeze casting with various bioceramics. **a** Hydroxyapatite, HA [31]. **b** Biphasic calcium phosphate, BCP [115]. **c** Alumina,  $\text{Al}_2\text{O}_3$  [79]. **d** Bioactive glass,

13–93 BG [151]. **e** HA-collagen freeze-cast composite [160]. **f**  $\text{ZrO}_2$  infiltrated with polymer epoxy [130]. Images adapted with permission

loadings using HA have ranged from 5 volume % (vol%) up to 45 vol%, with total porosity negatively correlating to the solid loading [62]. Sintering procedures often involve heating the green body up to at least 850 °C. Decomposition into  $\alpha$ -tricalcium phosphate [ $\text{Ca}_3(\text{PO}_4)_2$ ] and tetracalcium phosphate [ $\text{Ca}_4(\text{PO}_4)_2\text{O}$ ] are reported to occur above 1250 °C [31, 98, 99], however, there are reports of successful freeze-cast HA scaffolds without decomposition when sintered up to 1375 °C [100] and 1450 °C [101]. When used with unidirectional freeze casting, compressive strengths have ranged from 0.5 to 145 MPa [31, 102]. This wide range can be attributed to differences processing parameters. Solid loading often provides the greatest influence, with higher solid loadings leading to greater strengths and lower porosities [1, 62]. Freeze-cast HA has shown great potential as a bone graft substitute. Unidirectional porous HA with pores averaging 300  $\mu\text{m}$  have been studied in vivo with animal models [103, 104] and clinical cases [96, 105] with success in orthopedic applications [106] and Japanese Pharmaceuticals and Medical Devices Agency (PMDA) approval for use in human cases [107].

Tricalcium phosphate (TCP) [ $\text{Ca}_3(\text{PO}_4)_2$ ] is a biocompatible calcium phosphate similar to HA. TCP is commonly used in its  $\beta$ -TCP form and permanently transforms into a more soluble  $\alpha$ -TCP form when sintered above 1250 °C [93, 98]. Both forms of TCP are used in medical and dental applications [108]. One benefit of  $\beta$ -TCP over HA is its improved osteoinductivity, with many reports on successful osteoinduction through its usage [109]. While also readily accepted by the body, TCP resorbs much faster than HA, with partial resorption occurring within ten weeks [95, 110] and full resorption of a porous  $\beta$ -TCP implant occurring within 1–1.5 years leading to potential implant loosening [106, 111]. Along with faster resorption, TCP exhibits lower mechanical strength, which can limit the material's use in loading applications [110, 112]. When used with unidirectional freeze casting, scaffolds made from  $\beta$ -TCP had compressive strengths ranging from 0.1 to 45 MPa, again often determined by the solid loadings which ranged from 2 vol% up to 45 vol% [62]. Freeze-cast  $\beta$ -TCP scaffolds have been studied and have shown success in vivo with bone growth occurring in animal models [111]. They have also been

used in human studies for tibial reconstructions [113] and have achieved Japanese PMDA approval [114]. When compared to  $\beta$ -TCP scaffolds with spherically shaped pores, it was shown that the unidirectionally aligned pores offered by freeze-cast  $\beta$ -TCP scaffolds improved blood flow, cell attachment, and resource transportation [113].

Through combining HA and  $\beta$ -TCP, biphasic calcium phosphate (BCP) (Fig. 3b) has also been studied with freeze casting [115–117]. BCP takes advantage of the stability and strength of HA and the improved osteoinductivity and faster resorption of  $\beta$ -TCP. Because of its dual composition, BCP resorbs with an intermediate rate between its constituents but offers greater osteoinduction than HA [89]. Mechanical strengths of unidirectional, freeze-cast BCP scaffolds were reported from 0.02 to 36.4 MPa [116, 117]. Using a BCP composition of 20 weight % (wt%) HA to 80 wt%  $\beta$ -TCP, Yang et al. [116] showed suitable cytocompatibility with rat mesenchymal stem cells (MSCs), showing promise for future freeze-cast BCP research.

Fluoridation through partial and full substitution of the hydroxyl group in HA with fluorine can yield fluorohydroxyapatite (FHA) [ $\text{Ca}_{10}(\text{PO}_4)_6(\text{OH})_x\text{F}_{1-x}$ ] and fluorapatite (FA) [ $\text{Ca}_{10}(\text{PO}_4)_6\text{F}_2$ ], respectively [118, 119]. When compared to HA, FHA and FA have shown improved cell proliferation and differentiation [119, 120]. Fluoridation also provides thermal stability, allowing FHA and FA to be sintered at much higher temperatures (up to 1450 °C) than HA and  $\beta$ -TCP with notably less decomposition [121, 122]. Unidirectional, freeze-cast FHA scaffolds with 10 vol.% solid loading were reported to have compressive strengths ranging from 4.5 to 13.5 MPa depending on sintering temperature [123]. Through in vitro cell culturing, osteoblast cell proliferation increased with sintering temperature. While no freeze casting with FA has been reported so far, FA has become a steadily increasing subject of biomaterials research and freeze-cast FA could show promise for bone graft substitutes [124, 125].

## Bioinert Ceramics

Bioinert ceramics such as alumina ( $\text{Al}_2\text{O}_3$ ) (Fig. 3c), titania ( $\text{TiO}_2$ ), and zirconia ( $\text{ZrO}_2$ ) often exhibit different properties when compared to CPs such as: greater corrosion resistance, greater mechanical strength, and reduced cell activity [108, 126, 127]. In the pursuit of porous materials, freeze-casting research with these ceramics often focuses on other applications such as insulators and energy storage [61]. However, there are still reports for their use as biomaterials [128–131]. Reported freeze-casting compressive strengths are 1–25, 1–175, and 4.36–150.6 MPa for  $\text{TiO}_2$ ,  $\text{Al}_2\text{O}_3$ , and  $\text{ZrO}_2$ , respectively [62]. These mechanical properties show potential uses in both load-bearing and unloaded

regions. However, due to their biological inertness and lack of resorption, these materials often require additional processing to be suitable for use as bone graft substitutes, lest they face fibrous encapsulation [127].

Another factor to consider is the sintering behaviors of the materials. For freeze-cast scaffolds with the greatest strength,  $\text{TiO}_2$  completely transitions from anatase to rutile when sintered above 700 °C [132] versus alumina which requires sintering from 1500 to 1800 °C [133] and zirconia which exhibits the greatest mechanical properties when sintered from 1400 to 1550 °C [134]. While bioinert ceramics have been heavily studied and implemented in other technologies, their use as bone graft substitutes made through freeze casting lacks the strong foundation in research when compared to CPs.

## Ceramic–Ceramic Composites

Given the unique properties of specific materials, there are reports of freeze casting with ceramic-ceramic composites and element doping to improve upon limitations of the original constituents. These composites and doping methods are similarly used in other fabrication techniques, showing potential avenues of study for improved freeze-cast bioceramics [135–137]. When combined with other ceramics or doped with metal ions, CPs with improved properties have been achieved. One example would be the aforementioned BCP, using a combination of HA and  $\beta$ -TCP. Using a bioinert ceramic, Ghazanfari and Zamanian researched the influence of  $\text{Al}_2\text{O}_3$  concentrations on HA, showing greater mechanical strength and changes to the pore microstructure in freeze-cast HA- $\text{Al}_2\text{O}_3$  scaffolds because of the smaller  $\text{Al}_2\text{O}_3$  particle size [138]. When HA was combined with barium titanate ( $\text{BaTiO}_3$ ), an electrically active and biocompatible ceramic, human osteosarcoma MG-63 cells were better able to adhere to, proliferate on, and differentiate on the freeze-cast HA- $\text{BaTiO}_3$  scaffolds when compared to basic freeze-cast HA scaffolds [139]. Nanosized silica (silicon dioxide,  $\text{SiO}_2$ ), another biocompatible ceramic, added to freeze-cast HA scaffolds during freezing improved MG-63 cell proliferation and differentiation because the  $\text{SiO}_2$  altered the surface properties by providing bone nucleation sites through silanol ( $\text{Si-OH}$ ) groups; greater thermal stability was also observed with less shrinkage occurring from  $\text{SiO}_2$  presence [140]. Freeze-cast scaffolds made with more complex composite ceramics such as hardystonite ( $\text{Ca}_2\text{ZnSi}_2\text{O}_7$ ) [141] and merwinite ( $\text{Ca}_3\text{Mg}(\text{SiO}_4)_2$ ) [142] have also been studied for use as biomaterials. By doping CPs with strontium, Sr [143], and magnesium, Mg [144], or  $\text{Al}_2\text{O}_3$  with silicon [145], scaffolds with improved mechanical properties and bioactivity can be fabricated. Given the decomposition of CPs at high temperatures, large concentrations of a material that require higher sintering temperatures such as  $\text{Al}_2\text{O}_3$

could be detrimental to the desired product. Therefore, compatibility between the composite constituents must be considered to produce a viable bone graft substitute. Sintering may also lead to new, less desirable phases from decomposition, so the study of the sintering behavior should also be performed when using composites.

As another type of composite material, bioactive glasses (BGs) (Fig. 3d) are silicon-based, surface-reactive biomaterials with compositions mostly containing silica ( $\text{SiO}_2$ ). Depending on the product, they can also contain calcium oxide (CaO), sodium oxide ( $\text{Na}_2\text{O}$ ), phosphorus pentoxide ( $\text{P}_2\text{O}_5$ ), and additional oxides [32, 146]. Bioactive glass has garnered interest for bone repair due to its aptitude for cell growth, tissue attachment, and osteogenic potential [32, 147]. Another distinction of BGs are their antimicrobial properties, reducing the risk of biofilm production [148]. In vitro testing with freeze-cast scaffolds using BG 13-93 showed increasing cell proliferation over a period of 7 days, with cell activity observable within the depths of the scaffolds [149]. Similarly, freeze-cast BG scaffolds were seeded and implanted into rat models and were reported to produce tissue formation as well as the presence of HA on the surface of the scaffold [150]. Long term observations of in vivo animal models showed a change from brittle to elastic–plastic mechanical behavior after 24 weeks, indicating the potential for freeze-cast BG scaffolds to be used in load-bearing regions [151].

### Ceramic–Polymer Composites

In addition to ceramic–ceramic composites, freeze casting has also been used to fabricate ceramic–polymer composites. Both synthetic and natural polymers have been used, such as collagen, gelatin, chitosan, polyvinyl alcohol (PVA), and poly(methyl methacrylate) (PMMA) [152–155]. One benefit of polymer incorporation includes better compositional alignment with natural bone, which itself is a composite made from collagen, carbonated HA, water, and additional extracellular proteins. Another benefit of polymer incorporation is the improved cell growth shown in vitro on a CP-collagen scaffold when compared to only a CP one [156].

There are two main methods of polymer incorporation into freeze-cast bioceramics: slurry-based and infiltration-based. Slurry-based composites (Fig. 3e) incorporate the polymer into the initial slurry composition before freezing. These composites typically do not go through a sintering process to prevent the desired polymer from burning off [157]. While the mechanical strength is often less than that seen in sintered scaffolds, slurry-based composites often exhibit similar mechanical behavior to trabecular bone, moving from brittle to ductile failure with the inclusion of the polymer phase [158–160]. Yunoki et al. demonstrated in vivo tissue ingrowth into an HA-collagen slurry-based

composite scaffold in an 80–20 wt% composition [160]. These composite scaffolds exhibited viscoelastic behavior, with shape-recovery occurring after cyclic compression in addition to improved mechanical strength along the freezing direction. Furthermore, as mentioned previously with Tanaka et al. [34], the anisotropic pore structure provided by freeze casting allowed for improved tissue ingrowth when compared to randomly oriented, interconnected pores.

The polymer phase also offers the opportunity to improve osteoinduction by attaching growth factors much more easily or immobilizing them in the polymer phase during freezing. Many techniques have been produced that have successfully attached growth factors to polymer surfaces or embedded them into the polymer [161, 162]. While chemical attachment on CPs and other bioceramics is possible, there still remain some obstacles to overcome when compared to polymer functionalization [163]. Accordingly, further research into improving osteoinduction in freeze-cast ceramic–polymer scaffolds should be considered.

In contrast with slurry-based composites that add the polymer phase during the initial process, infiltration-based composites (Fig. 3f) add the polymer phase after the freeze-cast bioceramics has been sintered and densified. In doing so, the mechanical strength of the ceramic is preserved because of the sintering step while allowing the addition of a polymer or epoxy through infiltration into the pores. This infiltration step typically occurs by placing the scaffold into a polymer solution. While under vacuum, the material is percolated into the ceramic scaffold, either filling up the pores or coating the walls. Inversely of note, a slurry-based ceramic coating on a freeze-cast polymer scaffold with a ceramic composition of up to 45% was demonstrated by Wu et al. [164].

These infiltration-based composites offer many benefits, greatly improving mechanical strength and mimicking nacre or bone with high toughness [76, 112]. During crack formation in a fully infiltrated composite, the polymer has been reported to fill in the crack, thus improving the mechanical toughness [112, 165]. While porosity is lost through this infiltration, there still remains the potential for use as a bone graft substitute for load-bearing applications where dense cortical bone is desired [155, 166, 167]. In some cases, with proper dehydration to remove the solvent, porosity can be maintained with the polymer only coating the walls [112, 165]. This still allows for the movement of cells and vascularization. In vivo testing in Wistar rat cranial bone showed improved osteoblast density on polymer-coated scaffolds when compared to uncoated ones [112].

As a whole, freeze casting with bioceramics has heavily focused on HA,  $\beta$ -TCP, and BGs, with growing interest in ceramic–polymer composites, and with more limited research into bioinert ceramics. Trends toward further augmenting these freeze-cast bioceramics have focused on

composite fabrication with goals for improving mechanical performance, controlling resorption and degradation, and providing drug delivery and growth factor capabilities [69, 162, 168].

## Tailored Freeze-Cast Pore Structures

As a multi-step process, freeze casting offers many forms of control. During the freeze-casting process, both intrinsic and extrinsic controls can be used. Control of sintering also plays a role with improving mechanical properties. Additionally, freeze casting can be combined with other advanced manufacturing processes to produce unique pore structures.

### Uniform Pore Structure Controls (Intrinsic Controls)

Intrinsic control during the freezing process is typically seen while using unidirectional freezing (freezing along a single direction, often vertically) to limit the variables to control (Fig. 4). This control method affords a uniform pore structure. The most common and simplest way to control the uniform pore structure is through particle solid loading. Increasing solid loading is shown to negatively correlate with porosity, with higher solid loadings leading to denser materials as demonstrated with a variety of ceramic materials [31, 61, 62]. However, solid loading was shown to have no effect on pore size or scaffold wall thickness which can be controlled through other means [169, 170]. It is interesting to note that while porosity is negatively correlated to the mechanical strength, pore size and the resultant wall thickness are not. Instead, wall thickness was found to predict failure by Weibull modulus, with a higher probability of failure occurring within thick-walled pore structures because there were more regions for catastrophic failures [169]. However, because pore size and porosity are important for bone ingrowth, efforts should still be taken to ensure an appropriate pore structure without compromising mechanical strength.

Another method to modify the pore size is to adjust the slurry composition based on solvents (Fig. 4a) and additives. While water is the most common solvent because of its ease of access and biocompatibility, alternatives such as camphene [75] and tertiary-butyl alcohol (TBA) [101] have been used to provide different pore structures. The pore structure provided through freezing water is typically lamellar, with an initially dense region close to the initial freezing region [31]. Camphene ( $C_{10}H_{16}$ ), cyclohexane ( $C_6H_{12}$ ), and 1,4-dioxane ( $C_4H_8O_2$ ) are aromatic ring-based solvents that freeze above room temperature and can produce dendritic pores with greater branching occurring for a more complex pore structure [62, 171]. Honeycomb-shaped pores can be produced through freezing TBA ( $C_4H_{10}O$ ) and 1,4-dioxane

[62, 70, 172]. While pores made through freeze casting are often below 100  $\mu m$  [62], there have been notable successes in creating pores suitable for bone growth when using water, camphene, or 1,4-dioxane with pores ranging from 100 to 300  $\mu m$  [35, 62, 173].

In efforts to increase pore size and potentially improve mechanical strength, an annealing process of the solvents after they have been fully solidified has shown success [75, 174, 175]. This annealing process is reported to increase pore size and improve pore uniformity by coarsening dendritic structures, which is especially apparent when using a non-aqueous solvent like camphene that generates highly dendritic pores [75]. Understandably, this annealing process proves useful in providing a controllable pore structure as needed for bone graft substitutes and could develop into a useful step in the freezing process for freeze-cast bioceramics.

In efforts to mimic bone's various porous structures, a variety of additives have been studied for their effect on pore structure (Fig. 4b). Hydrogen peroxide and other evaporative chemicals have been used to produce spherical pores [176]. Alcohols are commonly used to induce larger pores as seen with isopropyl alcohol and ethanol [71, 177, 178]. Other materials like glycerol [126, 173], gelatin [69, 179], chitosan [179], and salts like sodium chloride [115] have been used to modify pore structures and sizes as well. These additives work by affecting the freezing kinetics through alterations to the freezing front and ice crystallization [1]. Mechanical properties can be changed too through pore structure alterations based on solvent choice. Fu et al. [100] compared how additions of glycerol and 1,4-dioxane to water could alter mechanical responses when using a 20 vol.% HA solid loading. Glycerol increased dendritic bridging while dioxane led to larger and more cellular pores, and the mechanical performance was shown to improve with greater strengths and strains to failure closer to those of bone. As most of these freeze-casting additives are polymeric, they are burned off during sintering, and so they are expected to have little effect on the freeze-cast scaffolds' performance and biocompatibility. However, metal-doping or ceramic additives mentioned previously for composites do remain, and thus can affect scaffold performance. On the other hand where the scaffold is not sintered, the polymer additives could also be used as a part of the biomaterial in addition to its role in affecting freezing kinetics.

Another method to control the pore structure depends on the freeze front velocity (Fig. 4c), or the velocity at which the solid-liquid interface of the solvent moves. There exist two methods to control this velocity: the first uses a constant substrate freezing temperature while the second uses a constant freezing rate. In both cases, reducing the freeze front velocity has led to larger pore sizes and thicker walls [61, 70, 180]. While freeze front velocity

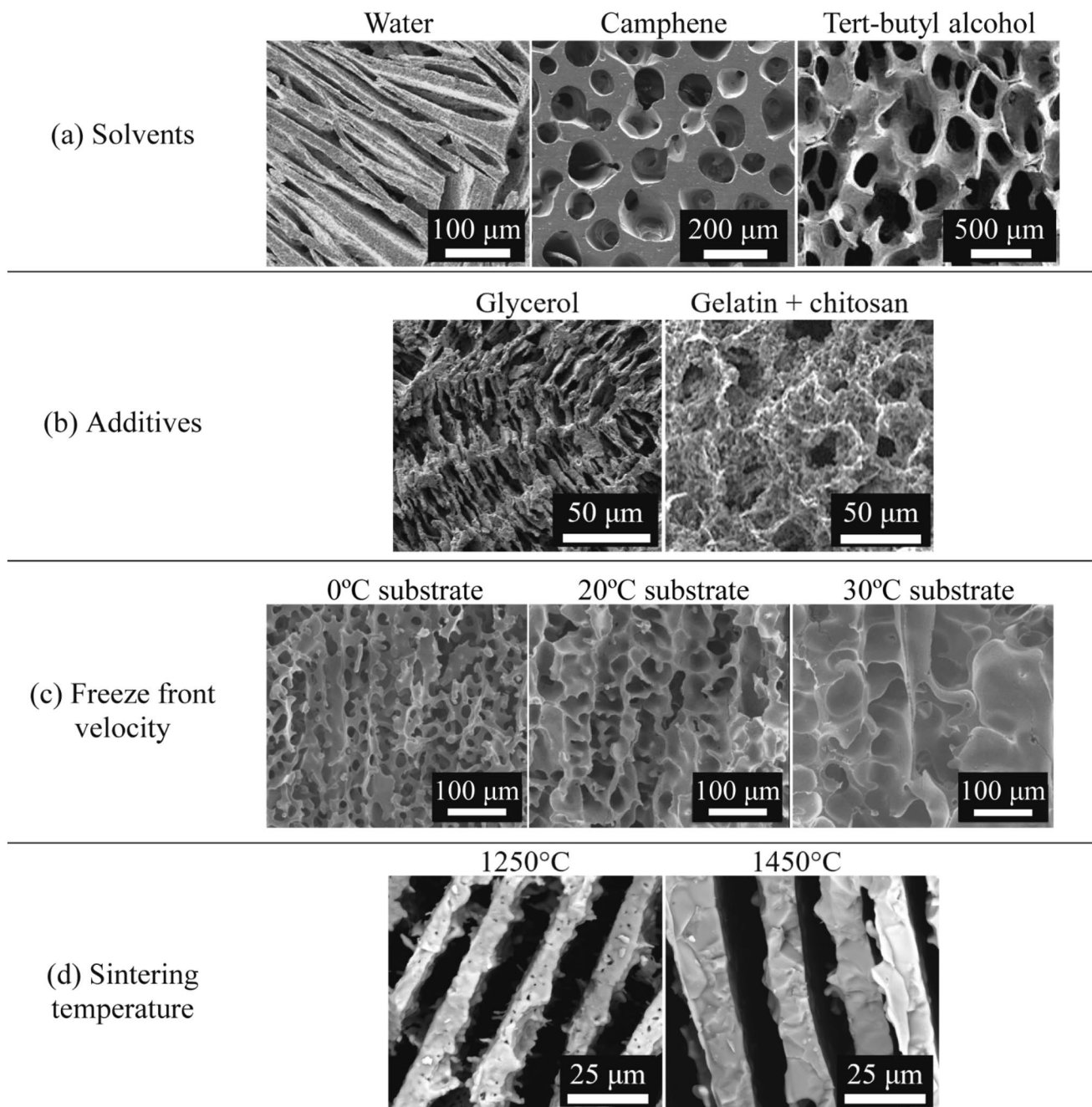


**Fig. 4** Microscopy images for intrinsic control methods for uniform pore structures in freeze-cast bioceramics. All images show the structure perpendicular to the freezing direction. **a** Solvents: (left to right) Water with HA-SiO<sub>2</sub> to produce lamellar pores [140], camphene with BG glass to produce columnar pores [75], TBA with HA to produce honeycomb pores [101]. **b** Additives: (left to right) 20 wt% glycerol

to HA in water [70], 1.5 wt% gelatin and 0.7 wt% chitosan to BPC in 0.5 M acetic acid [179]. **c** Freeze front velocity: decreasing freezing velocity through a warmer substrate temperature of HA in camphene to control pore size [180]. **d** Sintering: increasing sintering temperature for FHA to densify structure and improve mechanical strength [123]. Images adapted with permission

can control pore size and pore geometry based on the solvent, it holds little effect on the porosity, which is mainly influenced by solid loading [169]. With the ability to properly control the pore structure through intrinsic means, freeze casting has been proven to produce the pore sizes

necessary for proper cell proliferation [181]. This control over pore size, pore morphology, and porosity have been shown with a combination of multiple material, solvent, and additive combinations [62].

In addition to freezing parameters as uniform pore structure controls, sintering parameters can also be used. Sintering parameters mostly influence mechanical behavior with a more limited effect on the pore structure (Fig. 4d). While the many variables of the sintering profile can possibly influence the freeze-cast scaffold, the most common parameters that are studied are the dwell temperature and dwell time [100, 123, 182]. Freeze-cast scaffolds that have been sintered at higher temperatures or for longer time periods often demonstrated much greater mechanical properties with only slightly lower porosities [100, 123, 182]. Sintering of freeze-cast scaffolds can also affect the densification and surface characteristics of the material, with micropores appearing within walls at lower sintering temperatures [1, 123]. While there is much research on how sintering of freeze-cast bioceramics affects mechanical properties [62, 100], and research on how sintering of other bone replacements impacts *in vitro* bone growth has been done before [183–185], there is limited research on the biological impact of sintering behaviors for freeze-cast bioceramics [123]. Because sintering has been found to affect surface characteristics of porous scaffolds, which in turn affect bone growth [186], understanding and improving sintering procedures provides an avenue of study for freeze-cast bioceramics.

Exemplary detailed reports on these different uniform pore structure controls can be found in Fu et al. [70, 100] with their research focused on microstructure control and mechanical behavior. In their research on HA, Fu et al. explored various slurry compositions by adjusting solid loadings, introducing additives, and using different solvents. Additionally, they explored the effects of freeze front velocity and sintering temperatures. When examining mechanical behavior, they found that the freeze-cast HA exhibited high strain tolerance, high strain to failure, and high strain rate sensitivity [100]. In their works, Fu et al. have shown how uniform pore structure controls can be used to achieve the desired properties for a bone graft substitute.

### Localized Pore Structure Control (Extrinsic Controls)

Extrinsic control methods (Fig. 5) allow for the differentiation of localized pore structures and control over the shape of the biomaterial. Unidirectional freeze casting (Fig. 5a) with one temperature gradient often acts as the basis for more developed methods. One method to achieve this localized control is through templating or controlling the freezing parameters through physical means. While most freeze casting is performed with cylindrical molds, it can be used with a much wider range of geometries. By using a template or mold, a desired shape can be used to fit the needs of the application such as for a tibial wedge [113, 187]. Templating to control ice growth can also be achieved through the introduction of temperature gradients. Bai et al.

[76] demonstrated the use of bidirectional freeze casting by using a polydimethylsiloxane (PDMS) wedge to generate a highly aligned pore structure (Fig. 5b). The PDMS wedge introduced a second temperature gradient perpendicular to the first, leading to more aligned ice nucleation sites and hence aligned pores as seen in the electron microscopy image in Fig. 5b. This aligned pore structure could be useful in mimicking the orthotropic properties of bone. These scaffolds also resembled nacre when infiltrating the HA with an epoxy, producing a tough, lightweight, brick-and-mortar structure [155].

Shown in Fig. 5c, freeze-cast scaffolds with hierarchical structures through localized macropores can be generated by using a sacrificial template [77, 78]. Through additive manufacturing, a polymer or graphene oxide template with struts larger than 100  $\mu\text{m}$  can be placed into a freeze-cast slurry, where the freeze-cast pore structure will then be built around this template. As the green body is sintered, the polymer template will burn off, leaving a pore structure with micropores from freeze casting and macropores from the sacrificial template, a structure that would be difficult to achieve through other means. Similarly, Huang et al. [188] used reusable fibers that could be removed to create macropore channels, leading to a pore structure templated through ice and aligned fibers. While the mechanical performance of sacrificial template freeze-cast HA scaffolds was affected by the macropore size [77] or number of macropores [188], solid loading was still found to positively correlate with mechanical strength [78]. *In vitro* study found MG-63 cells proliferated well along the scaffolds, showing the potential of macro–micro porous freeze-cast scaffolds for bone growth through sacrificial templating [77].

Core–shell freeze casting (Fig. 5d) can be performed in multiple sequences to produce graded pore structures, similar to that of natural bone. These scaffolds are often fabricated using a smaller mold to create a porous core and this product is placed in a larger mold where the shell is then fabricated through freeze casting of a slurry with higher solid loading to create the dense shell [80, 171, 189]. The inverse can also be fabricated with a dense core and highly porous shell, which could prove useful in specific cases [171]. By mimicking the porous trabecular bone and dense cortical bone, maximum compressive strengths using HA were reported by Tang et al. and Lee et al. to be 22.2 MPa up to 47, respectively [80, 171]. When compared to regular unidirectional freeze-cast HA, the core–shell freeze-cast scaffolds maintained higher compressive strengths at similar porosities (i.e., solid loadings) [80]. Lee et al. attributed this improvement to the increase in buckling resistance provided by the denser shell. By increasing the ratio of the dense to porous area, mechanical strength in core–shell freeze-cast HA scaffolds was also found to range from 20 to 50 MPa [171]. This core–shell structure allowed for less total

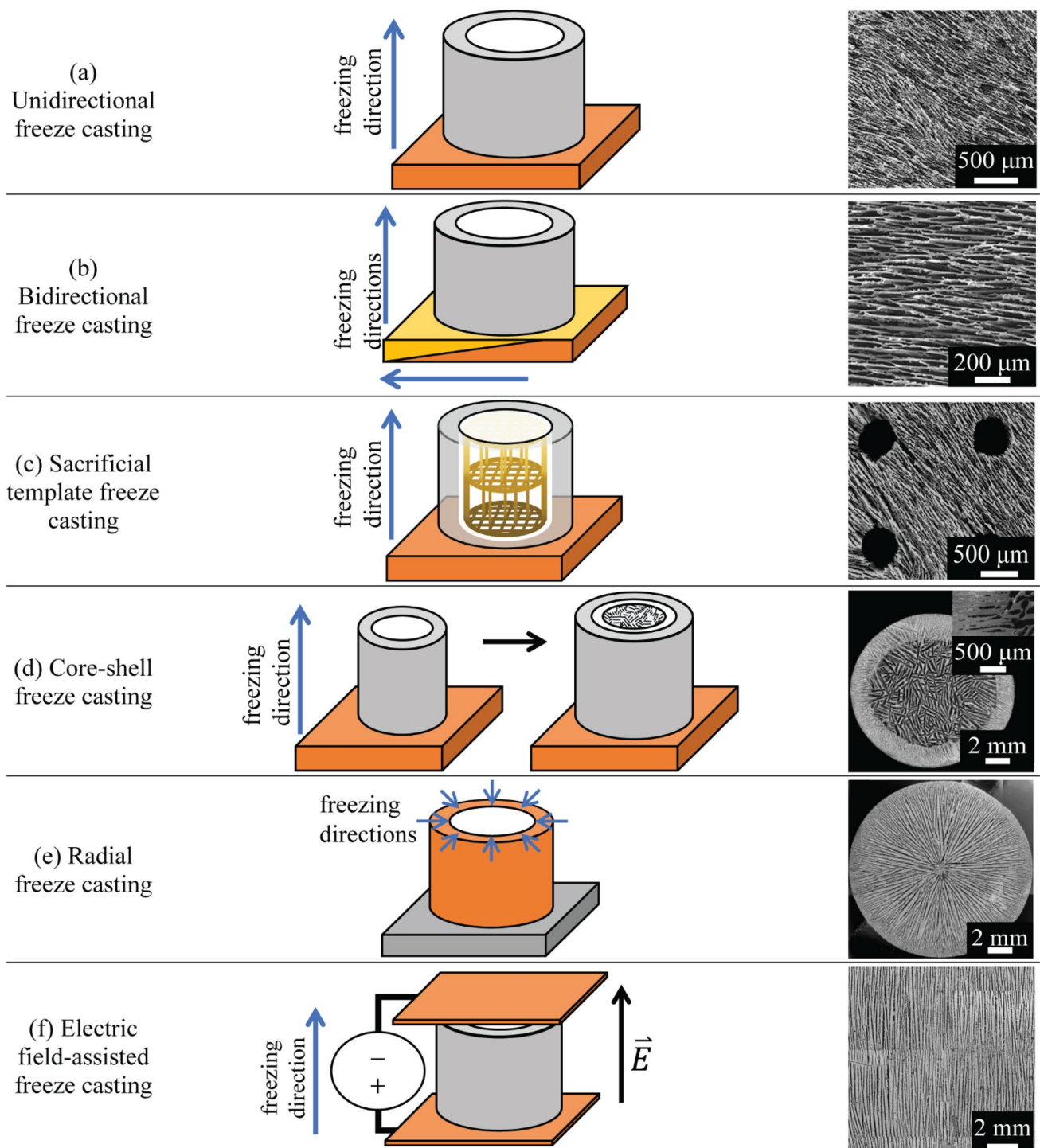


**Fig. 5** Illustrations (middle) and microscopy images (right) for extrinsic control methods for localized pore structures in freeze-cast bioceramics. Cross sections are perpendicular to the freezing direction (blue arrows). **a** Unidirectional freeze casting to produce a typical pore structure [77]. The metal cold finger (orange plate) leads to a vertical temperature gradient through the slurry (white ellipse) which is encased in an insulated mold (gray tube). **b** Bidirectional freeze casting with HA to produce a directionally aligned pore structure [155]. A horizontal temperature gradient is added through a polymer wedge (yellow wedge). **c** Sacrificial template freeze casting with HA to produce a hierarchical pore structure [77]. Note the template is

removed during the sintering step. **d** Core-shell freeze casting with HA to produce a core-shell pore structure [80]. Inset on microscopy image (upper right) shows a close-up of the interfacial pore structure from dense to porous regions from left to right. **e** Radial freeze casting with  $\text{Al}_2\text{O}_3$  to produce a centrosymmetric pore structure [190]. A metal mold (orange tube) creates a temperature gradient inward, leading to a radial temperature gradient. **f** Electric field-assisted freeze casting with  $\text{Al}_2\text{O}_3$  to produce directionally aligned pore structures [79]. In this orientation, the electric field is applied parallel to the freezing direction. Images adapted with permission

material to be used while achieving improved mechanical performance. In addition to improved mechanical properties, Lee et al. observed that these core–shell scaffolds also exhibited greater *in vitro* preosteoblast cell activity when compared to a  $\beta$ -TCP control [171]. However, as cortical bone requires much higher compressive strengths than those reported, this freeze-cast structure still has room for improvement before it can be used in load-bearing regions.

By changing the freezing direction, specific pore configurations can be fabricated. Radial symmetry through radial freeze casting (Fig. 5e) has been achieved with  $\text{Al}_2\text{O}_3$  [189–191] and HA [192] by using a thermally conductive mold, allowing ice crystals to nucleate along the cylindrical perimeter and freezing inwards. In a similar process, hollow, yttria-stabilized  $\text{ZrO}_2$  tubes were produced by rotating a chilled copper tube filled with slurry, producing a pore structure with a macroscopic hole in the center while the porous structure contained micropores from freeze casting [193]. Radial freeze casting has also been shown to produce a graded pore structure with pores up to 200  $\mu\text{m}$ , with a dense outer layer leading into a porous center, resembling the graded pore structure of bone [117, 192]. Going a step further, Su et al. [189] reported on the mechanical behavior of radial freeze casting of alumina combined with multiple freezing steps, leading to a dubbed “radial-concentric” freeze casting, mimicking the lamellar structure of cortical bone and other natural biological structures. When seeded with rat bone marrow MSCs *in vitro*, radial freeze-cast scaffolds were shown to produce a capillary flow because of the graded pore structure, mimicking the capillary action of bone [192]. While it is difficult to find radial symmetry in bone, the presence of biomimetic capillary action to aid cell growth [192] and mechanical properties comparable to trabecular bone [117] improves the viability of radial freeze-cast bioceramic scaffolds and could provide inspiration for other control methods.

While freeze casting with applied energetic fields such as ultrasonic [194], magnetic [82], and electric [79] fields have seen considerable research in thermal and energy applications, their study for use in biomaterials has been limited. Currently, only HA has been tested with electric field-assisted freeze casting for biomaterial applications, which produced different pore geometries with improved cell activity *in vitro* compared to scaffolds without an applied electric field [83]. However, reports on employing an electric field to  $\text{Al}_2\text{O}_3$  during freeze casting (Fig. 5f) showed that duration and strength of the electric field could induce a graded pore structure, increase dendritic bridging, and increase mechanical strength up to 118.7 MPa compared to control samples at 26.6 MPa [79, 85]. Given the higher mechanical strength requirements of cortical bone, combining electric field-assisted freeze casting with  $\text{Al}_2\text{O}_3$  may offer a solution for load-bearing regions using freeze-cast biomaterials. While there is a report on using

magnetic fields to control iron (II, III) oxide ( $\text{Fe}_3\text{O}_4$ ) added to HA,  $\text{Al}_2\text{O}_3$ ,  $\text{ZrO}_2$ , and  $\text{TiO}_2$ , the magnetic field had little influence on the bioceramics, instead the magnetic field caused distinct phase separation of the materials and  $\text{Fe}_3\text{O}_4$  [195]. As some bioinert ceramics such as  $\text{TiO}_2$  are paramagnetic, applying strong magnetic fields to produce aligned pore structures could eventually prove useful in creating freeze-cast biomaterials [67, 81]. Similarly, layered pore structures created through ultrasound freeze casting could mimic the laminar arrangement of osteons in bone [88]. Consequently, applied energetic fields offer conceivable benefits for freeze-cast bioceramics.

### Combined Freeze-Casting Fabrication

In addition to these control methods, there has recently been valuable research into fabrication processes that combine freeze casting with other advanced manufacturing processes for use as bone graft substitutes. Additive manufacturing with freeze casting has shown great potential, with the ability to create a tailored macrostructure while still maintaining the microporosity and mechanical strength required for bone growth. HA [196, 197],  $\text{SiO}_2$  [197], and akermanite ( $\text{Ca}_2\text{MgSi}_2\text{O}_7$ ) [198], all biocompatible materials, have been 3D-printed while in a slurry state before being frozen to produce a hierarchical porous structure. Similarly, a photocurable slurry containing CP was produced using camphene–camphor as the solvent, allowing for a digital light processing technique [199]. In these applications, freeze casting was used to produce micropores within the walls, while macropores could be produced through the additive manufacturing.

In a similar process to additive manufacturing, thin laminar layers of  $\text{Al}_2\text{O}_3$  slurry were frozen to provide uniquely shaped layered structures [200]. This cold slurry-based laminar object manufacturing could achieve 20° overhangs, showing the potential for use in fabricating bone graft substitutes to meet specific defect sites [200]. Additionally, two-dimensional shapes could be laser cut from the object, showing prospects in shaping a bone graft substitute to fit the treatment site.

While not using a laser to cut, Parandoush et al. produced a core–shell pore structure through freeze casting of HA followed by surface laser processing of the outer surface [201]. The laser processing provided a dense shell layer similar to cortical bone. Further testing should be done to determine the effect that this modification would have on mechanical properties. In brief, these reports of successful combinations of freeze casting and advanced manufacturing processes highlight the flexibility that freeze casting can provide for biomaterials.

## Conclusions and Future Prospects

In summary, research on freeze casting with bioceramics demonstrates substantial evidence toward the advancement of alloplastic bone graft substitutes. The major advantages of this technique are its versatility for material fabrication and many methods of structural control. Freeze casting has shown flexibility in working with a variety of biocompatible ceramic and ceramic composite materials with success *in vitro* and *in vivo* [106]. This technique's affinity with bioceramics means bone growth and osteoconduction are also achievable. Additionally, freeze-cast bioceramics have been fabricated with mechanical strengths suitable for both unloaded and load-bearing regions [113]. This mechanical strength is also attainable despite the need for a porous structure, for which pores larger than 100  $\mu\text{m}$  can be achieved with freeze casting. The essential porous structure can also be tailored to meet the orthotropic nature of bone through both uniform and localized control methods. Finally, the use of CPs can ensure a resorbable and biodegradable bone graft substitute. As such, freeze-cast bioceramics are highly suitable as potential bone graft substitutes.

Given the volume of research on freeze-cast bioceramics, it can be expected there will be continued interest in this avenue for biomaterial fabrication. One aspect to consider is the necessity of vascularization of a bone graft substitute, which has not been easily demonstrated or reported yet in a freeze-cast bioceramic. Similarly, research on osteoinduction, an imperative process in bone growth, in freeze-cast bioceramics is still lacking. Methods to provide vascularization and osteoinduction would prove fruitful in improving freeze casting for bone graft substitutes. Further study is needed as well to better understand and control how freeze-cast bioceramics are resorbed and how biodegradation progresses. Controlling the related properties of pore structure and mechanical strength still remains a challenge for freeze casting; however, the success of *in vivo* models provides an optimistic outlook for these bioceramics. Further research into composite materials is also aiding in the implementation of better matching the mechanical properties of bone. Lastly, as the role of growth factors, drug delivery, and other beneficial compounds on osteogenesis becomes better understood, their incorporation into freeze-cast bioceramics provides a promising opportunity for improvement.

**Acknowledgements** No funding is acknowledged for this work.

## Declarations

**Conflict of interest** The authors declare no conflict of interest.

## References

1. S. Deville, Freeze-casting of porous biomaterials: structure, properties and opportunities. *Materials* (Basel). **3**, 1913–1927 (2010). <https://doi.org/10.3390/ma3031913>
2. U.G.K. Wegst, M. Schecter, A. Donius, P. Hunger, Biomaterials by freeze casting. *Philos. Trans. A*. **368**, 2099–2121 (2010). <https://doi.org/10.1098/rsta.2010.0014>
3. I. Nelson, S.E. Naleway, Intrinsic and extrinsic control of freeze casting. *J. Market. Res.* **8**, 2372–2385 (2019). <https://doi.org/10.1016/j.jmrt.2018.11.011>
4. Q. Cheng, C. Huang, A.P. Tomsia, Freeze casting for assembling bioinspired structural materials. *Adv. Mater.* **29**, 1703155 (2017). <https://doi.org/10.1002/adma.201703155>
5. G. Shao, D.A.H. Hanaor, X. Shen, A. Gurlo, Freeze casting: from low-dimensional building blocks to aligned porous structures—a review of novel materials. *Methods Appl. Adv. Mater.* **32**, 1907176 (2020). <https://doi.org/10.1002/adma.201907176>
6. K. Qin, C. Parisi, F.M. Fernandes, Recent advances in ice templating: from biomimetic composites to cell culture scaffolds and tissue engineering. *J. Mater. Chem. B*. **9**, 889–907 (2021). <https://doi.org/10.1039/D0TB02506B>
7. Biosurgery Market - Global Forecast to 2026 | MarketsandMarkets (2022) <https://www.marketsandmarkets.com/Market-Reports/biosurgery-market-166922302.html>. Accessed 5 May 2022.
8. A.S. Greenwald, S.D. Boden, V.M. Goldberg, Y. Khan, C.T. Laurencin, R.N. Rosier, American Academy, of Orthopaedic Surgeons, The committee on biological implants, bone-graft substitutes: facts, fictions, and applications. *J. Bone Joint Surg. Am.* **83**, 98–103 (2001). <https://doi.org/10.2106/00004623-20010022-00007>
9. J.T.B. Ratnayake, M. Mucalo, G.J. Dias, Substituted hydroxyapatites for bone regeneration: a review of current trends. *J. Biomed. Mater. Res. Part B* **105**, 1285–1299 (2017). <https://doi.org/10.1002/jbm.b.33651>
10. R. Zhao, R. Yang, P.R. Cooper, Z. Khurshid, A. Shavandi, J. Ratnayake, Bone grafts and substitutes in dentistry: a review of current trends and developments. *Molecules* **26**, 3007 (2021). <https://doi.org/10.3390/molecules26103007>
11. Bone Grafts and Substitutes Market Report, 2022–2030 (2022) <https://www.grandviewresearch.com/industry-analysis/bone-grafts-substitutes-market>. Accessed 5 May 2022
12. Dental Bone Graft Substitute Market - Global Forecast to 2025 | MarketsandMarkets (2022). <https://www.marketsandmarkets.com/Market-Reports/dental-bone-graft-substitutes-market-159678690.html>. Accessed 5 May 2022
13. R.H. Gross, The use of bone grafts and bone graft substitutes in pediatric orthopaedics: an overview. *J. Pediatr. Orthopaed.* **32**, 100–105 (2012). <https://doi.org/10.1097/BPO.0b013e31823d8350>
14. Pediatric Orthopedic Implants Market Global Analysis to 2027, The Insight Partners. (n.d.). <https://www.theinsightpartners.com/reports/pediatric-orthopedic-implants-market>. Accessed 5 May 2022
15. H.J. Haugen, S.P. Lyngstadaas, F. Rossi, G. Perale, Bone grafts: which is the ideal biomaterial? *J. Clin. Periodontol.* **46**, 92–102 (2019). <https://doi.org/10.1111/jcpe.13058>
16. A. Kolk, J. Handschel, W. Drescher, D. Rothamel, F. Kloss, M. Blessmann, M. Heiland, K.-D. Wolff, R. Smeets, Current trends and future perspectives of bone substitute materials: from space holders to innovative biomaterials. *J. Cranio-Maxillofac. Surg.* **40**, 706–718 (2012). <https://doi.org/10.1016/j.jcms.2012.01.002>
17. P. Kazimierzczak, A. Przekora, Osteoconductive and osteoinductive surface modifications of biomaterials for bone regeneration:

- a concise review. *Coatings* **10**, 971 (2020). <https://doi.org/10.3390/coatings10100971>
18. B. Huzum, B. Puha, R.M. Necoara, S. Gheorghievici, G. Puha, A. Filip, P.D. Sirbu, O. Alexa, Biocompatibility assessment of biomaterials used in orthopedic devices: an overview (review). *Exp. Ther. Med.* **22**, 1–9 (2021). <https://doi.org/10.3892/etm.2021.10750>
  19. ISO 10993-1:2018(en), Biological evaluation of medical devices—part 1: evaluation and testing within a risk management process, (n.d.). <https://www.iso.org/obp/ui/#iso:std:iso:10993:-1:ed-5:v2:en>. Accessed 25 May 2022
  20. T. Albrektsson, C. Johansson, Osteoinduction, osteoconduction and osseointegration. *Eur Spine J.* **10**, S96–S101 (2001). <https://doi.org/10.1007/s005860100282>
  21. J.L. Drago, J.Y. Choi, J.R. Lieberman, J. Huang, P.A. Zuk, J. Zhang, M.H. Hedrick, P. Benhaim, Bone induction by BMP-2 transduced stem cells derived from human fat. *J. Orthop. Res.* **21**, 622–629 (2003). [https://doi.org/10.1016/S0736-0266\(02\)00238-3](https://doi.org/10.1016/S0736-0266(02)00238-3)
  22. H. Egusa, W. Sonoyama, M. Nishimura, I. Atsuta, K. Akiyama, Stem cells in dentistry: part I: stem cell sources. *J. Prosthodont. Res.* **56**, 151–165 (2012). <https://doi.org/10.1016/j.jpor.2012.06.001>
  23. Y. Suzawa, N. Kubo, S. Iwai, Y. Yura, H. Ohgushi, M. Akashi, Biomineral/agarose composite gels enhance proliferation of mesenchymal stem cells with osteogenic capability. *Int. J. Mol. Sci.* **16**, 14245–14258 (2015). <https://doi.org/10.3390/ijms160614245>
  24. Y. Fillingham, J. Jacobs, Bone grafts and their substitutes. *Bone Joint J.* **98**, 6–9 (2016). <https://doi.org/10.1302/0301-620X.98B.36350>
  25. K.S. Katti, Biomaterials in total joint replacement. *Colloids Surf. B* **39**, 133–142 (2004). <https://doi.org/10.1016/j.colsurfb.2003.12.002>
  26. A. Dehghanhadikolaei, B. Fotovvati, Coating techniques for functional enhancement of metal implants for bone replacement: a review. *Materials*. **12**, 1795 (2019). <https://doi.org/10.3390/ma12111795>
  27. Y.-C. Fung, Bone and cartilage, in *Biomechanics: mechanical properties of living tissues*. ed. by Y.-C. Fung (Springer, New York, 1993)
  28. T. Kokubo, H.-M. Kim, M. Kawashita, Novel bioactive materials with different mechanical properties. *Biomaterials* **24**, 2161–2175 (2003). [https://doi.org/10.1016/s0142-9612\(03\)00044-9](https://doi.org/10.1016/s0142-9612(03)00044-9)
  29. M. Amaral, M.A. Lopes, R.F. Silva, J.D. Santos, Densification route and mechanical properties of Si<sub>3</sub>N<sub>4</sub>-bioglass biocomposites. *Biomaterials* **23**, 857–862 (2002). [https://doi.org/10.1016/s0142-9612\(01\)00194-6](https://doi.org/10.1016/s0142-9612(01)00194-6)
  30. P. Baldwin, D.J. Li, D.A. Auston, H.S. Mir, R.S. Yoon, K.J. Koval, Autograft, allograft, and bone graft substitutes: clinical evidence and indications for use in the setting of orthopaedic trauma surgery. *J. Orthop. Trauma* **33**, 203–213 (2019). <https://doi.org/10.1097/BOT.0000000000001420>
  31. S. Deville, E. Saiz, A.P. Tomsia, Freeze casting of hydroxyapatite scaffolds for bone tissue engineering. *Biomaterials* **27**, 5480–5489 (2006). <https://doi.org/10.1016/j.biomaterials.2006.06.028>
  32. G. Iviglia, S. Kargozar, F. Baino, Biomaterials, current strategies, and novel nano-technological approaches for periodontal regeneration. *J. Funct. Biomater.* **10**, 3 (2019). <https://doi.org/10.3390/jfb10010003>
  33. J.R. Woodard, A.J. Hilldore, S.K. Lan, C.J. Park, A.W. Morgan, J.A.C. Eurell, S.G. Clark, M.B. Wheeler, R.D. Jamison, A.J. Wagoner Johnson, The mechanical properties and osteoconductivity of hydroxyapatite bone scaffolds with multi-scale porosity. *Biomaterials* **28**, 45–54 (2007). <https://doi.org/10.1016/j.biomaterials.2006.08.021>
  34. M. Tanaka, H. Haniu, T. Kamanaka, T. Takizawa, A. Sobajima, K. Yoshida, K. Aoki, M. Okamoto, H. Kato, N. Saito, Physicochemical, in vitro, and in vivo evaluation of a 3D unidirectional porous hydroxyapatite scaffold for bone regeneration. *Materials (Basel)*. **10**, 33 (2017). <https://doi.org/10.3390/ma10010033>
  35. Y. Suetsugu, Y. Hotta, M. Iwasashi, M. Sakane, M. Kikuchi, T. Ikoma, T. Higaki, N. Ochiai, M. Tanaka, Structural and tissue reaction properties of novel hydroxyapatite ceramics with unidirectional pores. *Key Eng. Mater.* **330–332**, 1003–1006 (2007). <https://doi.org/10.4028/www.scientific.net/KEM.330-332.1003>
  36. S. Overgaard, M. Lind, K. Josephsen, A.B. Maunsbach, C. Bünger, K. Søballe, Resorption of hydroxyapatite and fluorapatite ceramic coatings on weight-bearing implants: a quantitative and morphological study in dogs. *J. Biomed. Mater. Res.* **39**, 141–152 (1998). [https://doi.org/10.1002/\(SICI\)1097-4636\(199801\)39:1%3c141::AID-JBM16%3e3.0.CO;2-I](https://doi.org/10.1002/(SICI)1097-4636(199801)39:1%3c141::AID-JBM16%3e3.0.CO;2-I)
  37. S. Liu, H. Zhou, H. Liu, H. Ji, W. Fei, E. Luo, Fluorine-contained hydroxyapatite suppresses bone resorption through inhibiting osteoclasts differentiation and function in vitro and in vivo. *Cell Prolif.* (2019). <https://doi.org/10.1111/cpr.12613>
  38. S.V. Dorozhkin, Dissolution mechanism of calcium apatites in acids: A review of literature. *World Journal of Methodology*. **2**, 1 (2012). <https://doi.org/10.5662/wjm.v2.i1.1>
  39. C.J. Tredwin, A.M. Young, E.A. Abou Neel, G. Georgiou, J.C. Knowles, Hydroxyapatite, fluor-hydroxyapatite and fluorapatite produced via the sol-gel method: dissolution behaviour and biological properties after crystallization. *J. Mater. Sci. Mater. Med.* **25**, 47–53 (2014). <https://doi.org/10.1007/s10856-013-5050-y>
  40. K.M.R. Nuss, B. von Rechenberg, Biocompatibility issues with modern implants in bone: a review for clinical orthopedics. *Open Orthop. J.* **2**, 66–78 (2008). <https://doi.org/10.2174/1874325000802010066>
  41. S. Christian, M. Doris, S. Alexis, L. Georgios, S. Else, K. Franz, D. Karl, E. Rolf, The fluorohydroxyapatite (FHA) FRIOS® Aligpore® is a suitable biomaterial for the reconstruction of severely atrophic human maxillae. *Clin. Oral Implant Res.* **14**, 743–749 (2003). <https://doi.org/10.1046/j.2003.00959.x>
  42. M. Roy, A. Bandyopadhyay, S. Bose, Ceramics in bone grafts and coated implants (n.d.) 52
  43. L. Guo, S. Ataollah Naghavi, Z. Wang, S. Nath Varma, Z. Han, Z. Yao, L. Wang, L. Wang, C. Liu, On the design evolution of hip implants: a review. *Mater. Des.* (2022). <https://doi.org/10.1016/j.matdes.2022.110552>
  44. S.E.C.M. van de Vijfeijken, T.J.A.G. Múnker, R. Spijker, L.H.E. Karssemakers, W.P. Vandertop, A.G. Becking, D.T. Ubbink, A.G. Becking, L. Dubois, L.H.E. Karssemakers, D.M.J. Milstein, S.E.C.M. van de Vijfeijken, P.R.A.M. Depauw, F.W.A. Hoefnagels, W.P. Vandertop, C.J. Kleverlaan, T.J.A.G. Múnker, T.J.J. Maal, E. Nout, M. Riool, S.A.J. Zaat, Autologous bone is inferior to alloplastic cranioplasties: safety of autograft and allograft materials for cranioplasties, a systematic review. *World Neurosurg.* **117**, 443–452.e8 (2018). <https://doi.org/10.1016/j.wneu.2018.05.193>
  45. R.B. Osman, M.V. Swain, A critical review of dental implant materials with an emphasis on titanium versus zirconia. *Materials (Basel)*. **8**, 932–958 (2015). <https://doi.org/10.3390/ma8030932>
  46. R.A. Bhatt, T.D. Rozental, Bone graft substitutes. *Hand Clin.* **28**, 457–468 (2012). <https://doi.org/10.1016/j.hcl.2012.08.001>
  47. G. Fernandez de Grado, L. Keller, Y. Idoux-Gillet, Q. Wagner, A.-M. Musset, N. Benkirane-Jessel, F. Bornert, D. Offner, Bone substitutes: a review of their characteristics, clinical use, and

- perspectives for large bone defects management. *J. Tissue Eng.* (2018). <https://doi.org/10.1177/2041731418776819>
48. J.H. Lee, G.S. Yi, J.W. Lee, D.J. Kim, Physicochemical characterization of porcine bone-derived grafting material and comparison with bovine xenografts for dental applications. *J. Periodontal Implant Sci.* **47**, 388–401 (2017). <https://doi.org/10.5051/jpis.2017.47.6.388>
  49. C.T. Laurencin, S.F. El-Amin, Xenotransplantation in orthopaedic surgery. *JAAOS* **16**, 4–8 (2008)
  50. I. Pountos, P.V. Giannoudis, Is there a role of coral bone substitutes in bone repair? *Injury* **47**, 2606–2613 (2016). <https://doi.org/10.1016/j.injury.2016.10.025>
  51. F. Gashtasbi, S. Hasannia, S. Hasannia, M. Mahdi Dehghan, F. Sarkarat, A. Shali, Comparative study of impact of animal source on physical, structural, and biological properties of bone xenograft. *Xenotransplantation* **27**, 12628 (2020). <https://doi.org/10.1111/xen.12628>
  52. R. Nicholas, Ethical considerations in allograft tissue transplantation: a surgeon's perspective. *Clin. Orthop. Relat. Res.* **435**, 11–16 (2005). <https://doi.org/10.1097/01.blo.0000165734.41886.19>
  53. L. Luzzi, A.J. Spencer, Factors influencing the use of public dental services: an application of the theory of planned behaviour. *BMC Health Serv. Res.* **8**, 93 (2008). <https://doi.org/10.1186/1472-6963-8-93>
  54. C. Bucchi, M. del Fabbro, A. Arias, R. Fuentes, J.M. Mendes, M. Ordonneau, V. Orti, M.-C. Manzanares-Céspedes, Multicenter study of patients' preferences and concerns regarding the origin of bone grafts utilized in dentistry. *Patient Prefer Adherence.* **13**, 179–185 (2019). <https://doi.org/10.2147/PPA.S186846>
  55. A.S. Almutairi, A descriptive analysis of patient's preferences in bone graft therapy in dentistry. *Int. J. Health Sci. (Qassim)* **13**, 24–28 (2019)
  56. I.-H. Jo, K.-H. Shin, Y.-M. Soon, Y.-H. Koh, J.-H. Lee, H.-E. Kim, Highly porous hydroxyapatite scaffolds with elongated pores using stretched polymeric sponges as novel template. *Mater. Lett.* **63**, 1702–1704 (2009). <https://doi.org/10.1016/j.matlet.2009.05.017>
  57. M.-S. Kim, I.-H. Park, B.-T. Lee, Fabrication and characterization of porous hydroxyapatite scaffolds. *Korean J. Mater. Res.* **19**, 680–685 (2009). <https://doi.org/10.3740/MRSK.2009.19.12.680>
  58. J. Kim, D. Lim, Y.H. Kim, K. Young-Hag, M.H. Lee, I. Han, S.J. Lee, O.S. Yoo, H.-S. Kim, J.-C. Park, A comparative study of the physical and mechanical properties of porous hydroxyapatite scaffolds fabricated by solid freeform fabrication and polymer replication method. *Int. J. Precis. Eng. Manuf.* **12**, 695–701 (2011). <https://doi.org/10.1007/s12541-011-0090-z>
  59. U. Deisinger, S. Hamisch, M. Schumacher, F. Uhl, R. Detsch, G. Ziegler, Fabrication of tailored hydroxyapatite scaffolds: comparison between a direct and an indirect rapid prototyping technique. *Key Eng. Mater.* **361–363**, 915–918 (2008). <https://doi.org/10.4028/www.scientific.net/KEM.361-363.915>
  60. C.E. Wilson, J.D. de Bruijn, C.A. van Blitterswijk, A.J. Verbout, W.J.A. Dhert, Design and fabrication of standardized hydroxyapatite scaffolds with a defined macro-architecture by rapid prototyping for bone-tissue-engineering research. *J. Biomed. Mater. Res. Part A* **68A**, 123–132 (2004). <https://doi.org/10.1002/jbm.a.20015>
  61. S. Deville, Ice-templating, freeze casting: beyond materials processing. *J. Mater. Res.* **28**, 2202–2219 (2013). <https://doi.org/10.1557/jmr.2013.105>
  62. K.L. Scotti, D.C. Dunand, Freeze casting: a review of processing, microstructure and properties via the open data repository FreezeCasting.net. *Progress Mater. Sci.* **94**, 243–305 (2018). <https://doi.org/10.1016/j.pmatsci.2018.01.001>
  63. T. Waschki, R. Oberacker, M.J. Hoffmann, Investigation of structure formation during freeze-casting from very slow to very fast solidification velocities. *Acta Mater.* **59**, 5135–5145 (2011). <https://doi.org/10.1016/j.actamat.2011.04.046>
  64. S. Deville, E. Maire, A. Lasalle, A. Bogner, C. Gauthier, J. Leloup, C. Guizard, In situ X-ray radiography and tomography observations of the solidification of aqueous alumina particle suspensions—part I: initial instants. *J. Am. Ceram. Soc.* **92**, 2489–2496 (2009). <https://doi.org/10.1111/j.1551-2916.2009.03163.x>
  65. A. Zamanian, S. Farhangdoust, M. Yasaei, M. Khorami, M. Hafezi, The effect of particle size on the mechanical and microstructural properties of freeze-casted macroporous hydroxyapatite scaffolds. *Int. J. Appl. Ceram. Technol.* **11**, 12–21 (2014). <https://doi.org/10.1111/jjac.12031>
  66. Z. Kaviani, A. Zamanian, Effect of nanohydroxyapatite addition on the pore morphology and mechanical properties of freeze cast hydroxyapatite scaffolds. *Proc. Mater. Sci.* **11**, 190–195 (2015). <https://doi.org/10.1016/j.mspro.2015.11.102>
  67. M.B. Frank, S. Hei Siu, K. Karandikar, C.-H. Liu, S.E. Naleway, M.M. Porter, O.A. Graeve, J. McKittrick, Synergistic structures from magnetic freeze casting with surface magnetized alumina particles and platelets. *J. Mech. Behav. Biomed. Mater.* **76**, 153–163 (2017). <https://doi.org/10.1016/j.jmbbm.2017.06.002>
  68. P.M. Hunger, A.E. Donius, U.G.K. Wegst, Platelets self-assemble into porous nacre during freeze casting. *J. Mech. Behav. Biomed. Mater.* **19**, 87–93 (2013). <https://doi.org/10.1016/j.jmbbm.2012.10.013>
  69. F. Ghorbani, H. Nojehdehian, A. Zamanian, Physicochemical and mechanical properties of freeze cast hydroxyapatite-gelatin scaffolds with dexamethasone loaded PLGA microspheres for hard tissue engineering applications. *Mater. Sci. Eng. C* **69**, 208–220 (2016). <https://doi.org/10.1016/j.msec.2016.06.079>
  70. Q. Fu, M.N. Rahaman, F. Dogan, B.S. Bal, Freeze casting of porous hydroxyapatite scaffolds. I. Processing and general microstructure. *J. Biomed. Mater. Res. Part B.* **86B**, 125–135 (2008). <https://doi.org/10.1002/jbm.b.30997>
  71. S.E. Naleway, C.F. Yu, R.L. Hsiung, A. Sengupta, P.M. Iovine, J.A. Hildebrand, M.A. Meyers, J. McKittrick, Bioinspired intrinsic control of freeze cast composites: harnessing hydrophobic hydration and clathrate hydrates. *Acta Mater.* **114**, 67–79 (2016). <https://doi.org/10.1016/j.actamat.2016.05.019>
  72. Y. Zhang, K. Zuo, Y.-P. Zeng, Effects of gelatin addition on the microstructure of freeze-cast porous hydroxyapatite ceramics. *Ceram. Int.* **35**, 2151–2154 (2009). <https://doi.org/10.1016/j.ceramint.2008.11.022>
  73. M.M. Porter, R. Imperio, M. Wen, M.A. Meyers, J. McKittrick, Bioinspired scaffolds with varying pore architectures and mechanical properties. *Adv. Func. Mater.* **24**, 1978–1987 (2014). <https://doi.org/10.1002/adfm.201302958>
  74. S. Deville, E. Saiz, A.P. Tomsia, Ice-templated porous alumina structures. *Acta Mater.* **55**, 1965–1974 (2007). <https://doi.org/10.1016/j.actamat.2006.11.003>
  75. X. Liu, M.N. Rahaman, Q. Fu, A.P. Tomsia, Porous and strong bioactive glass (13–93) scaffolds prepared by unidirectional freezing of camphene-based suspensions. *Acta Biomater.* **8**, 415–423 (2012). <https://doi.org/10.1016/j.actbio.2011.07.034>
  76. H. Bai, Y. Chen, B. Delattre, A.P. Tomsia, R.O. Ritchie, Bioinspired large-scale aligned porous materials assembled with dual temperature gradients. *Sci. Adv.* (2015). <https://doi.org/10.1126/sciadv.1500849>
  77. J.-Y. Jung, S.E. Naleway, Y.N. Maker, K.Y. Kang, J. Lee, J. Ha, S.S. Hur, S. Chien, J. McKittrick, 3D printed templating of extrinsic freeze-casting for macro-microporous biomaterials. *ACS Biomater. Sci. Eng.* **5**, 2122–2133 (2019). <https://doi.org/10.1021/acsbomaterials.8b01308>

78. Y.-M. Soon, K.-H. Shin, Y.-H. Koh, J.-H. Lee, W.-Y. Choi, H.-E. Kim, Fabrication and compressive strength of porous hydroxyapatite scaffolds with a functionally graded core/shell structure. *J. Eur. Ceram. Soc.* **31**, 13–18 (2011). <https://doi.org/10.1016/j.jeurceramsoc.2010.09.008>
79. Y. Tang, S. Qiu, Q. Miao, C. Wu, Fabrication of lamellar porous alumina with axisymmetric structure by directional solidification with applied electric and magnetic fields. *J. Eur. Ceram. Soc.* **36**, 1233–1240 (2016). <https://doi.org/10.1016/j.jeurceramsoc.2015.12.012>
80. Y. Tang, K. Zhao, L. Hu, Z. Wu, Two-step freeze casting fabrication of hydroxyapatite porous scaffolds with bionic bone graded structure. *Ceram. Int.* **39**, 9703–9707 (2013). <https://doi.org/10.1016/j.ceramint.2013.04.038>
81. I. Nelson, J. Varga, P. Wadsworth, M. Mroz, J.J. Kruzic, O.T. Kingstedt, S.E. Naleway, Helical and bouligand porous scaffolds fabricated by dynamic low strength magnetic field freeze casting. *JOM.* **72**, 1498–1508 (2020). <https://doi.org/10.1007/s11837-019-04002-9>
82. J.R. Fernquist, H.C. Fu, S.E. Naleway, Improved structural and mechanical performance of iron oxide scaffolds freeze cast under oscillating magnetic fields. *Ceram. Int.* **48**, 15034–15042 (2022). <https://doi.org/10.1016/j.ceramint.2022.02.032>
83. Z. Cheng, K. Zhao, Z.P. Wu, Structure control of hydroxyapatite ceramics via an electric field assisted freeze casting method. *Ceram. Int.* **41**, 8599–8604 (2015). <https://doi.org/10.1016/j.ceramint.2015.03.069>
84. J.E. John, S. Qian, D. Ghosh, Assembly of alumina particles in aqueous suspensions induced by high-frequency AC electric field. *J. Am. Ceram. Soc.* (2022). <https://doi.org/10.1111/jace.18527>
85. S. Akurati, S. Qian, D. Ghosh, AC electric field-assisted fabrication of ice-templated alumina materials and remarkable enhancement of compressive strength. *Scripta Mater.* (2022). <https://doi.org/10.1016/j.scriptamat.2021.114264>
86. A.K. Sánchez-Hernández, J. Martínez-Juárez, J.J. Gervacio-Arciniega, R. Silva-González, M.J. Robles-Águila, Effect of ultrasound irradiation on the synthesis of hydroxyapatite/titanium oxide nanocomposites. *Curr. Comput.-Aided Drug Des.* **10**, 959 (2020). <https://doi.org/10.3390/cryst10110959>
87. T.A. Ogden, M. Prisbrey, I. Nelson, B. Raeymaekers, S.E. Naleway, Ultrasound freeze casting: Fabricating bioinspired porous scaffolds through combining freeze casting and ultrasound directed self-assembly. *Mater. Des.* (2019). <https://doi.org/10.1016/j.matdes.2018.107561>
88. M. Mroz, J.L. Rosenberg, C. Acevedo, J.J. Kruzic, B. Raeymaekers, S.E. Naleway, Ultrasound freeze-casting of a biomimetic layered microstructure in epoxy-ceramic composite materials to increase strength and hardness. *Materialia.* (2020). <https://doi.org/10.1016/j.mtla.2020.100754>
89. S.R. Dutta, D. Passi, P. Singh, A. Bhuibhar, Ceramic and non-ceramic hydroxyapatite as a bone graft material: a brief review. *Ir. J. Med. Sci.* **184**, 101–106 (2015). <https://doi.org/10.1007/s11845-014-1199-8>
90. D.R. Bienek, D. Skrtic, Utility of amorphous calcium phosphate-based scaffolds in dental/biomedical applications. *Biointerface Res. Appl. Chem.* **7**, 1989–1994 (2017)
91. H. Yuan, M. van den Doel, S. Li, C. Blitterswijk, K. Groot, J. de Bruijn, A comparison of the osteoinductive potential of two calcium phosphate ceramics implanted intramuscularly in goats. *J. Mater. Sci. Mater. Med.* **13**, 1271–1275 (2003). <https://doi.org/10.1023/A:1021191432366>
92. M. Zhou, Y. Geng, S. Li, X. Yang, Y. Che, J.L. Pathak, G. Wu, Nanocrystalline hydroxyapatite-based scaffold adsorbs and gives sustained release of osteoinductive growth factor and facilitates bone regeneration in mice ectopic model. *J. Nanomater.* (2019). <https://doi.org/10.1155/2019/1202159>
93. J.S. Al-Sanabani, A.A. Madfa, F.A. Al-Sanabani, Application of calcium phosphate materials in dentistry. *Int. J. Biomater.* (2013). <https://doi.org/10.1155/2013/876132>
94. Z. Tang, X. Li, Y. Tan, H. Fan, X. Zhang, The material and biological characteristics of osteoinductive calcium phosphate ceramics. *Regen Biomater.* **5**, 43–59 (2018). <https://doi.org/10.1093/rb/rbx024>
95. Z. Sheikh, M.-N. Abdallah, A.A. Hanafi, S. Misbahuddin, H. Rashid, M. Glogauer, Mechanisms of in vivo degradation and resorption of calcium phosphate based biomaterials. *Materials (Basel).* **8**, 7913–7925 (2015). <https://doi.org/10.3390/ma8115430>
96. K. Demiya, T. Kunisada, E. Nakata, J. Hasei, T. Ozaki, Regeneration of the fibula with unidirectional porous hydroxyapatite. *Case Rep. Orthop.* (2019). <https://doi.org/10.1155/2019/9024643>
97. A.J. Tonino, B.C.H. van der Wal, I.C. Heyligers, B. Grimm, Bone remodeling and hydroxyapatite resorption in coated primary hip prostheses. *Clin Orthop Relat Res.* **467**, 478–484 (2009). <https://doi.org/10.1007/s11999-008-0559-y>
98. S.-F. Ou, S.-Y. Chiou, K.-L. Ou, Phase transformation on hydroxyapatite decomposition. *Ceram. Int.* **39**, 3809–3816 (2013). <https://doi.org/10.1016/j.ceramint.2012.10.221>
99. L. Pejchalová, J. Roleček, D. Salamon, Why freeze-casting brings different phase composition of calcium phosphates? *Open Ceram.* (2021). <https://doi.org/10.1016/j.oceram.2021.100161>
100. Q. Fu, M.N. Rahaman, F. Dogan, B.S. Bal, Freeze casting of porous hydroxyapatite scaffolds. II. Sintering, microstructure, and mechanical behavior. *J. Biomed. Mater. Res. B.* **86**, 514–522 (2008). <https://doi.org/10.1002/jbm.b.31051>
101. T.Y. Yang, J.M. Lee, S.Y. Yoon, H.C. Park, Hydroxyapatite scaffolds processed using a TBA-based freeze-gel casting/polymer sponge technique. *J. Mater. Sci.* **21**, 1495–1502 (2010). <https://doi.org/10.1007/s10856-010-4000-1>
102. K. Zhou, Y. Zhang, D. Zhang, X. Zhang, Z. Li, G. Liu, T.W. Button, Porous hydroxyapatite ceramics fabricated by an ice-templating method. *Scripta Mater.* **64**, 426–429 (2011). <https://doi.org/10.1016/j.scriptamat.2010.11.001>
103. M. Iwasashi, T. Funayama, A. Watanabe, H. Noguchi, T. Tsukanishi, Y. Suetsugu, T. Makihara, N. Ochiai, M. Yamazaki, M. Sakane, Bone regeneration and remodeling within a unidirectional porous hydroxyapatite bone substitute at a cortical bone defect site: histological analysis at one and two years after implantation. *Materials.* **8**, 4884–4894 (2015). <https://doi.org/10.3390/ma8084884>
104. M. Iwasashi, M. Sakane, Y. Suetsugu, N. Ochiai, Bone regeneration at cortical bone defect with unidirectional porous hydroxyapatite in vivo. *Key Eng. Mater.* **396–398**, 11–14 (2009). <https://doi.org/10.4028/www.scientific.net/KEM.396-398.11>
105. K. Uemura, A. Kanamori, K. Aoto, M. Yamazaki, M. Sakane, Novel unidirectional porous hydroxyapatite used as a bone substitute for open wedge high tibial osteotomy. *J. Mater. Sci. - Mater. Med.* **25**, 2541–2547 (2014). <https://doi.org/10.1007/s10856-014-5266-5>
106. T. Funayama, H. Noguchi, H. Kumagai, K. Sato, T. Yoshioka, M. Yamazaki, Unidirectional porous beta-tricalcium phosphate and hydroxyapatite artificial bone: a review of experimental evaluations and clinical applications. *J. Artif. Organs.* **24**, 103–110 (2021). <https://doi.org/10.1007/s10047-021-01270-8>
107. Approval for Prosthetic Bone Implants Obtained (Kuraray Medical Inc.) | kuraray, (n.d.). <https://www.kuraray.com/news/2009/090820> (accessed May 31, 2022).
108. M.-P. Ginebra, M. Espanol, Y. Maazouz, V. Bergez, D. Pastorino, Bioceramics and bone healing. *EFORT Open Rev.* **3**, 173–183 (2018). <https://doi.org/10.1302/2058-5241.3.170056>

109. M. Bohner, B.L.G. Santoni, N. Döbelin,  $\beta$ -tricalcium phosphate for bone substitution: synthesis and properties. *Acta Biomater.* **113**, 23–41 (2020). <https://doi.org/10.1016/j.actbio.2020.06.022>
110. A. Ogose, T. Hotta, H. Kawashima, N. Kondo, W. Gu, T. Kamura, N. Endo, Comparison of hydroxyapatite and beta tricalcium phosphate as bone substitutes after excision of bone tumors. *J. Biomed. Mater. Res.* **72B**, 94–101 (2005). <https://doi.org/10.1002/jbm.b.30136>
111. H. Kumagai, M. Iwasashi, T. Funayama, S. Nakamura, H. Noguchi, M. Koda, M. Yamazaki, Surgical repair of acetabular fracture using unidirectional porous  $\beta$ -tricalcium phosphate. *Case Rep. Orthop.* **2019**, 6860591 (2019). <https://doi.org/10.1155/2019/6860591>
112. T. Furusawa, T. Minatoya, T. Okudera, Y. Sakai, T. Sato, Y. Matsushima, H. Unuma, Enhancement of mechanical strength and in vivo cytocompatibility of porous  $\beta$ -tricalcium phosphate ceramics by gelatin coating. *Int. J. Implant Dentistry.* **2**, 4 (2016). <https://doi.org/10.1186/s40729-016-0037-3>
113. N. Kikuchi, T. Yoshioka, Y. Taniguchi, A. Kanamori, M. Yamazaki, Use of unidirectional and spherical porous  $\beta$ -tricalcium phosphate in opening-wedge high tibial osteotomy: a case series. *J Rural Med.* **16**, 52–55 (2021). <https://doi.org/10.2185/jrm.2020-007>
114. Kuraray to Release AFFINOS Bioresorbable Bone-graft Substitute | kuraray (n.d.) <https://www.kuraray.com/news/2015/151027>. Accessed 31 May 2022
115. F. He, Y. Yang, J. Ye, Tailoring the pore structure and property of porous biphasic calcium phosphate ceramics by NaCl additive. *Ceram. Int.* **42**, 14679–14684 (2016). <https://doi.org/10.1016/j.ceramint.2016.06.092>
116. Y. Yang, F. He, J. Ye, Preparation, mechanical property and cytocompatibility of freeze-cast porous calcium phosphate ceramics reinforced by phosphate-based glass. *Mater. Sci. Eng. C* **69**, 1004–1009 (2016). <https://doi.org/10.1016/j.msec.2016.08.008>
117. A. Macchetta, I.G. Turner, C.R. Bowen, Fabrication of HA/TCP scaffolds with a graded and porous structure using a camphene-based freeze-casting method. *Acta Biomater.* **5**, 1319–1327 (2009). <https://doi.org/10.1016/j.actbio.2008.11.009>
118. J. Chen, Z. Yu, P. Zhu, J. Wang, Z. Gan, J. Wei, Y. Zhao, S. Wei, Effects of fluorine on the structure of fluorohydroxyapatite: a study by XRD, solid-state NMR and Raman spectroscopy. *J. Mater. Chem. B.* **3**, 34–38 (2015). <https://doi.org/10.1039/C4TB01561D>
119. B.T. Bennett, J.P. Beck, K. Papangkorn, J.S. Colombo, K.N. Bachus, J. Agarwal, J.F. Shieh, S. Jeyapalina, Characterization and evaluation of fluoridated apatites for the development of infection-free percutaneous devices. *Mater. Sci. Eng. C Mater. Biol. Appl.* **100**, 665–675 (2019). <https://doi.org/10.1016/j.msec.2019.03.025>
120. A. Elghazel, R. Taktak, J. Bouaziz, S.C. and H. Keskes, TCP-fluorapatite composite scaffolds: mechanical characterization and in vitro/in vivo testing. *Scaffolds Tissue Eng.* (2017). <https://doi.org/10.5772/intechopen.69852>
121. Y. Chen, X. Miao, Thermal and chemical stability of fluorohydroxyapatite ceramics with different fluorine contents. *Biomaterials* **26**, 1205–1210 (2005). <https://doi.org/10.1016/j.biomaterials.2004.04.027>
122. H. Qu, M. Wei, Effect of fluorine content on mechanical properties of sintered fluoridated hydroxyapatite. *Mater. Sci. Eng., C* **26**, 46–53 (2006). <https://doi.org/10.1016/j.msec.2005.06.005>
123. T.J. Yin, S. Jeyapalina, S.E. Naleway, Characterization of porous fluorohydroxyapatite bone-scaffolds fabricated using freeze casting. *J. Mech. Behav. Biomed. Mater.* (2021). <https://doi.org/10.1016/j.jmbbm.2021.104717>
124. S. Jeyapalina, E. Hillas, J.P. Beck, J. Agarwal, J. Shea, Fluorapatite and fluorohydroxyapatite apatite surfaces drive adipose-derived stem cells to an osteogenic lineage. *J. Mech. Behav. Biomed. Mater.* (2022). <https://doi.org/10.1016/j.jmbbm.2021.104950>
125. R. Taktak, A. Elghazel, J. Bouaziz, S. Charfi, H. Keskes, Tricalcium phosphate-Fluorapatite as bone tissue engineering: evaluation of bioactivity and biocompatibility. *Mater. Sci. Eng., C* **86**, 121–128 (2018). <https://doi.org/10.1016/j.msec.2017.11.011>
126. K.K. Mallick, Freeze casting of porous bioactive glass and bio-ceramics. *J. Am. Ceram. Soc.* **92**, S85–S94 (2009). <https://doi.org/10.1111/j.1551-2916.2008.02784.x>
127. C. Piconi, S. Sprio, Oxide bioceramic composites in orthopedics and dentistry. *J. Compos. Sci.* **5**, 206 (2021). <https://doi.org/10.3390/jcs5080206>
128. H. Yoon, H. Choe, H. Choi, A morphological study on the titanium-oxide foams processed using freeze-casting. *J. Korean Ceram. Soc.* **49**, 427–431 (2012). <https://doi.org/10.4191/kcers.2012.49.5.427>
129. J. Li, K. Zuo, W. Liu, Y. Zeng, F. Zhang, D. Jiang, Porous  $\text{Al}_2\text{O}_3$  prepared via freeze casting and its biocompatibility. *Ceram. Trans.* **210**, 537–543 (2010). <https://doi.org/10.1002/9780470640845.ch76>
130. S.E. Naleway, K.C. Fickas, Y.N. Maker, M.A. Meyers, J. McKittrick, Reproducibility of  $\text{ZrO}_2$ -based freeze casting for biomaterials. *Mater. Sci. Eng. C* **61**, 105–112 (2016). <https://doi.org/10.1016/j.msec.2015.12.012>
131. W. Li, K. Lu, J. Walz, Freeze casting of porous materials: review of critical factors in microstructure evolution. *Int. Mater. Rev.* **57**, 37–60 (2012). <https://doi.org/10.1179/1743280411Y.0000000011>
132. C. Byrne, R. Fagan, S. Hinder, D.E. McCormack, S.C. Pillai, New approach of modifying the anatase to rutile transition temperature in  $\text{TiO}_2$  photocatalysts. *RSC Adv.* **6**, 95232–95238 (2016). <https://doi.org/10.1039/C6RA19759K>
133. A.R. Olszyna, P. Marchlewski, K.J. Kurzydowski, Sintering of high-density, high-purity alumina ceramics. *Ceram. Int.* **23**, 323–328 (1997). [https://doi.org/10.1016/S0272-8842\(96\)00031-4](https://doi.org/10.1016/S0272-8842(96)00031-4)
134. B. Stawarczyk, M. Ozcan, L. Hallmann, A. Ender, A. Mehl, C.H.F. Hämmerlet, The effect of zirconia sintering temperature on flexural strength, grain size, and contrast ratio. *Clin. Oral Investig.* **17**, 269–274 (2013). <https://doi.org/10.1007/s00784-012-0692-6>
135. R. Comín, M.P. Cid, L. Grinschpun, C. Oldani, N.A. Salvatierra, Titanium-hydroxyapatite composites sintered at low temperature for tissue engineering: in vitro cell support and biocompatibility. *J. Appl. Biomater. Funct. Mater.* **15**, e176–e183 (2017). <https://doi.org/10.5301/jabfm.5000340>
136. E.A. Abou Neel, J.C. Knowles, Physical and biocompatibility studies of novel titanium dioxide doped phosphate-based glasses for bone tissue engineering applications. *J. Mater. Sci.* **19**, 377–386 (2008). <https://doi.org/10.1007/s10856-007-3079-5>
137. Y. Luo, D. Li, J. Zhao, Z. Yang, P. Kang, In vivo evaluation of porous lithium-doped hydroxyapatite scaffolds for the treatment of bone defect. *Biomed. Mater. Eng.* **29**, 699–721 (2018). <https://doi.org/10.3233/BME-181018>
138. S.M.H. Ghazanfari, A. Zamanian, Phase transformation, microstructural and mechanical properties of hydroxyapatite/alumina nanocomposite scaffolds produced by freeze casting, (2013). <http://www.sciencedirect.com/science/article/pii/S0272884213006123>. Accessed 6 Aug 2018
139. Y. Zhang, Y.X. Bao, K.C. Zhou, D. Zhang, Fabrication of barium titanate/hydroxyapatite with aligned pore channels by freeze casting. *Appl. Mech. Mater.* **692**, 341–346 (2014). <https://doi.org/10.4028/www.scientific.net/AMM.692.341>

140. Z.-Q. Jia, Z.-X. Guo, F. Chen, J.-J. Li, L. Zhao, L. Zhang, Microstructure, phase compositions and in vitro evaluation of freeze casting hydroxyapatite-silica scaffolds. *Ceram. Int.* **44**, 3636–3643 (2018). <https://doi.org/10.1016/j.ceramint.2017.11.114>
141. M. Azizi, M. Kalantar, N. Nezafati, A. Zamanian, Fabrication, characterization, and in vitro bioactivity evaluation of freeze-cast highly porous hardystonite ceramic reinforced by graphene oxide as a novel bone scaffold. *J. Aust. Ceram. Soc.* **57**, 947–960 (2021). <https://doi.org/10.1007/s41779-021-00601-5>
142. N. Nezafati, M. Hafezi, A. Zamanian, M. Naserirad, Effect of adding nano-titanium dioxide on the microstructure, mechanical properties and in vitro bioactivity of a freeze cast merwinite scaffold. *Biotechnol. Prog.* **31**, 550–556 (2015). <https://doi.org/10.1002/btpr.2042>
143. E. Landi, F. Valentini, A. Tampieri, Freeze-casting of biomimetic apatites for the development of scaffolds. *J. Appl. Biomater. Biomech.* **8**, 119–119 (2010). <https://doi.org/10.1177/228080001000800223>
144. L.-K. Yang, Q. Jin, R.-F. Guo, P. Shen, Bio-inspired lamellar hydroxyapatite/magnesium composites prepared by directional freezing and pressureless infiltration. *Ceram. Int.* **47**, 11183–11192 (2021). <https://doi.org/10.1016/j.ceramint.2020.12.242>
145. M.E. Launey, E. Munch, D.H. Alsem, E. Saiz, A.P. Tomsia, R.O. Ritchie, A novel biomimetic approach to the design of high-performance ceramic–metal composites. *J. R. Soc. Interface.* **7**, 741–753 (2010). <https://doi.org/10.1098/rsif.2009.0331>
146. F04 Committee F1583-03, Specification for glass and glass ceramic biomaterials for implantation. *ASTM Int.* (2017). <https://doi.org/10.1520/F1538-03R17>
147. L.L. Hench, *Bioceramics*. *J. Am. Ceram. Soc.* **81**, 1705–1728 (1998). <https://doi.org/10.1111/j.1151-2916.1998.tb02540.x>
148. L. Drago, M. Toscano, M. Bottagisio, Recent evidence on bioactive glass antimicrobial and antibiofilm activity: a mini-review. *Materials (Basel)*. **11**, 326 (2018). <https://doi.org/10.3390/ma11020326>
149. Q. Fu, M.N. Rahaman, B.S. Bal, W. Huang, D.E. Day, Preparation and bioactive characteristics of a porous 13–93 glass, and fabrication into the articulating surface of a proximal tibia. *J. Biomed. Mater. Res. Part A* **82A**, 222–229 (2007). <https://doi.org/10.1002/jbm.a.31156>
150. X. Liu, M.N. Rahaman, Q. Fu, Bone regeneration in strong porous bioactive glass (13–93) scaffolds with an oriented microstructure implanted in rat calvarial defects. *Acta Biomater.* **9**, 4889–4898 (2013). <https://doi.org/10.1016/j.actbio.2012.08.029>
151. Q. Fu, M.N. Rahaman, B.S. Bal, K. Kuroki, R.F. Brown, In vivo evaluation of 13–93 bioactive glass scaffolds with trabecular and oriented microstructures in a subcutaneous rat implantation model. *J. Biomed. Mater. Res. A*. **95**, 235–244 (2010). <https://doi.org/10.1002/jbm.a.32827>
152. Y.B. Pottathara, T. Vuherer, U. Maver, V. Kokol, Morphological, mechanical, and in-vitro bioactivity of gelatine/collagen/hydroxyapatite based scaffolds prepared by unidirectional freeze-casting. *Polym. Test.* (2021). <https://doi.org/10.1016/j.polymertesting.2021.107308>
153. S.K. Swain, D. Sarkar, Fabrication, bioactivity, in vitro cytotoxicity and cell viability of cryo-treated nanohydroxyapatite–gelatin–polyvinyl alcohol macroporous scaffold. *J. Asian Ceram. Soc.* **2**, 241–247 (2014). <https://doi.org/10.1016/j.jascer.2014.05.003>
154. A. Rogina, P. Rico, G. Gallego Ferrer, M. Ivanković, H. Ivanković, Effect of in situ formed hydroxyapatite on microstructure of freeze-gelled chitosan-based biocomposite scaffolds. *Eur. Polym. J.* **68**, 278–287 (2015). <https://doi.org/10.1016/j.eurpolymj.2015.05.004>
155. H. Bai, F. Walsh, B. Gludovatz, B. Delattre, C. Huang, Y. Chen, A.P. Tomsia, R.O. Ritchie, Bioinspired hydroxyapatite/poly(methyl methacrylate) composite with a nacre-mimetic architecture by a bidirectional freezing method. *Adv. Mater.* **28**, 50–56 (2016). <https://doi.org/10.1002/adma.201504313>
156. Z. Xia, X. Yu, X. Jiang, H.D. Brody, D.W. Rowe, M. Wei, Fabrication and characterization of biomimetic collagen–apatite scaffolds with tunable structures for bone tissue engineering. *Acta Biomater.* **9**, 7308–7319 (2013). <https://doi.org/10.1016/j.actbio.2013.03.038>
157. E. Landi, F. Valentini, A. Tampieri, Porous hydroxyapatite/gelatine scaffolds with ice-designed channel-like porosity for biomedical applications. *Acta Biomater.* **4**, 1620–1626 (2008). <https://doi.org/10.1016/j.actbio.2008.05.023>
158. S. Yunoki, T. Ikoma, A. Monkawa, E. Marukawa, S. Sotome, K. Shinomiya, J. Tanaka, Three-dimensional porous hydroxyapatite/collagen composite with rubber-like elasticity. *J. Biomater. Sci. Polym. Ed.* **18**, 393–409 (2007). <https://doi.org/10.1163/156856207780425077>
159. S. Yunoki, T. Ikoma, A. Monkawa, K. Ohta, M. Kikuchi, S. Sotome, K. Shinomiya, J. Tanaka, Control of pore structure and mechanical property in hydroxyapatite/collagen composite using unidirectional ice growth. *Mater. Lett.* **60**, 999–1002 (2006). <https://doi.org/10.1016/j.matlet.2005.10.064>
160. S. Yunoki, T. Ikoma, A. Tsuchiya, A. Monkawa, K. Ohta, S. Sotome, K. Shinomiya, J. Tanaka, Fabrication and mechanical and tissue ingrowth properties of unidirectionally porous hydroxyapatite/collagen composite. *J. Biomed. Mater. Res. B* **80B**, 166–173 (2007). <https://doi.org/10.1002/jbm.b.30581>
161. A. Haider, S. Haider, S. Soo Han, I.-K. Kang, Recent advances in the synthesis, functionalization and biomedical applications of hydroxyapatite: a review. *RSC Adv.* **7**, 7442–7458 (2017). <https://doi.org/10.1039/C6RA26124H>
162. F. Ghorbani, B. Ghalandari, M. Sahranavard, A. Zamanian, M.N. Collins, Tuning the biomimetic behavior of hybrid scaffolds for bone tissue engineering through surface modifications and drug immobilization. *Mater. Sci. Eng., C* (2021). <https://doi.org/10.1016/j.msec.2021.112434>
163. A.K. Teotia, D.B. Raina, C. Singh, N. Sinha, H. Isaksson, M. Tägil, L. Lidgren, A. Kumar, Nano-hydroxyapatite bone substitute functionalized with bone active molecules for enhanced cranial bone regeneration. *ACS Appl. Mater. Interfaces* **9**, 6816–6828 (2017). <https://doi.org/10.1021/acsami.6b14782>
164. M. Wu, F. Chen, P. Wu, Z. Yang, S. Zhang, L. Xiao, Z. Deng, C. Zhang, Y. Chen, L. Cai, Bioinspired redwood-like scaffolds coordinated by in situ-generated silica-containing hybrid nano-coatings promote angiogenesis and osteogenesis both in vitro and in vivo. *Adv. Healthcare Mater.* **10**, 2101591 (2021). <https://doi.org/10.1002/adhm.202101591>
165. X. Qi, J. Ye, Y. Wang, Alginate/poly (lactic-co-glycolic acid)/calcium phosphate cement scaffold with oriented pore structure for bone tissue engineering. *J. Biomed. Mater. Res. Part A* **89A**, 980–987 (2009). <https://doi.org/10.1002/jbm.a.32054>
166. E. Munch, M.E. Launey, D.H. Alsem, E. Saiz, A.P. Tomsia, R.O. Ritchie, Tough, bio-inspired hybrid materials. *Science* **322**, 1516–1520 (2008). <https://doi.org/10.1126/science.1164865>
167. S. Lee, M. Porter, S. Wasko, G. Lau, P.-Y. Chen, E.E. Novitskaya, A.P. Tomsia, A. Almutairi, M.A. Meyers, J. McKittrick, Potential bone replacement materials prepared by two methods. *MRS Proc.* **1418**, 12 (2012). <https://doi.org/10.1557/opl.2012.671>
168. S.-H. Jun, E.-J. Lee, T.-S. Jang, H.-E. Kim, J.-H. Jang, Y.-H. Koh, Bone morphogenic protein-2 (BMP-2) loaded hybrid coating on porous hydroxyapatite scaffolds for bone tissue engineering. *J. Mater. Sci.* **24**, 773–782 (2013). <https://doi.org/10.1007/s10856-012-4822-0>
169. J. Seuba, S. Deville, C. Guizard, A.J. Stevenson, The effect of wall thickness distribution on mechanical reliability and strength

- in unidirectional porous ceramics. *Sci. Technol. Adv. Mater.* **17**, 128–135 (2016). <https://doi.org/10.1080/14686996.2016.1140309>
170. J. Seuba, S. Deville, C. Guizard, A.J. Stevenson, Mechanical properties and failure behavior of unidirectional porous ceramics. *Sci. Rep.* **6**, 24326 (2016). <https://doi.org/10.1038/srep24326>
  171. H. Lee, T.-S. Jang, J. Song, H.-E. Kim, H.-D. Jung, The production of porous hydroxyapatite scaffolds with graded porosity by sequential freeze-casting. *Materials*. **10**, 367 (2017). <https://doi.org/10.3390/ma10040367>
  172. J.H. Kim, J.H. Lee, T.Y. Yang, S.Y. Yoon, B.K. Kim, H.C. Park, TBA-based freeze/gel casting of porous hydroxyapatite scaffolds. *Ceram. Int.* **37**, 2317–2322 (2011). <https://doi.org/10.1016/j.ceramint.2011.03.023>
  173. Q. Fu, M.N. Rahaman, F. Dogan, B.S. Bal, Freeze-cast hydroxyapatite scaffolds for bone tissue engineering applications. *Biomed. Mater.* (2008). <https://doi.org/10.1088/1748-6041/3/2/025005>
  174. Y. Tang, M. Mao, S. Qiu, C. Wu, Annealing effects on the pore structures and mechanical properties of porous alumina via directional freeze-casting. *J. Eur. Ceram. Soc.* **38**, 4149–4154 (2018). <https://doi.org/10.1016/j.jeurceramsoc.2018.04.038>
  175. K.M. Pawelec, A. Husmann, S.M. Best, R.E. Cameron, Altering crystal growth and annealing in ice-templated scaffolds. *J. Mater. Sci.* **50**, 7537–7543 (2015). <https://doi.org/10.1007/s10853-015-9343-z>
  176. Z. Cheng, K. Zhao, W. Zhang, C. Guo, Preparation of hydroxyapatite scaffolds via freeze-casting using hydrogen peroxide/distilled water. *J. Chin. Ceram. Soc.* **42**, 672–676 (2014). <https://doi.org/10.7521/j.issn.0454-5648.2014.05.19>
  177. A. Kumar, Y.S. Negi, V. Choudhary, N.K. Bhardwaj, Microstructural and mechanical properties of porous biocomposite scaffolds based on polyvinyl alcohol, nano-hydroxyapatite and cellulose nanocrystals. *Cellulose* **21**, 3409–3426 (2014). <https://doi.org/10.1007/s10570-014-0339-7>
  178. J. Zeng, Y. Zhang, K. Zhou, D. Zhang, Effects of alcohol additives on pore structure and morphology of freeze-cast ceramics. *Trans. Nonferrous Met. Soc. China* **24**, 718–722 (2014). [https://doi.org/10.1016/S1003-6326\(14\)63116-2](https://doi.org/10.1016/S1003-6326(14)63116-2)
  179. L.M. Henning, S. Zavareh, P.H. Kamm, M. Höner, H. Fischer, J. Banhart, F. Schmidt, A. Gurlo, Manufacturing and characterization of highly porous bioactive glass composite scaffolds using unidirectional freeze casting. *Adv. Eng. Mater.* **19**, 1700129 (2017). <https://doi.org/10.1002/adem.201700129>
  180. B.-H. Yoon, Y.-H. Koh, C.-S. Park, H.-E. Kim, Generation of large pore channels for bone tissue engineering using camphene-based freeze casting. *J. Am. Ceram. Soc.* **90**, 1744–1752 (2007). <https://doi.org/10.1111/j.1551-2916.2007.01670.x>
  181. T. Makihara, M. Sakane, H. Noguchi, T. Tsukanishi, Y. Suet-sugu, M. Yamazaki, Formation of osteon-like structures in unidirectional porous hydroxyapatite substitute. *J. Biomed. Mater. Res. B Appl. Biomater.* **106**, 2665–2672 (2018). <https://doi.org/10.1002/jbm.b.34083>
  182. A. Zamanian, S. Farhangdoust, M. Yasaei, M. Khorami, M. Abbasabadi, The effect of sintering temperature on the microstructural and mechanical characteristics of hydroxyapatite macroporous scaffolds prepared via freeze-casting. *Key Eng. Mater.* (2013). <https://doi.org/10.4028/www.scientific.net/KEM.529-530.133>
  183. A.-T. Xu, W.-T. Qi, M.-N. Lin, Y.-H. Zhu, F.-M. He, The optimization of sintering treatment on bovine-derived bone grafts for bone regeneration: in vitro and in vivo evaluation. *J. Biomed. Mater. Res. B* **108**, 272–281 (2020). <https://doi.org/10.1002/jbm.b.34387>
  184. J. Lu, M.-C. Blary, S. Vavasseur, M. Descamps, K. Anselme, P. Hardouin, Relationship between bioceramics sintering and micro-particles-induced cellular damages. *J. Mater. Sci. Mater. Med.* **15**, 361–365 (2004). <https://doi.org/10.1023/b:jmsm.0000021102.68509.65>
  185. E. Champion, Sintering of calcium phosphate bioceramics. *Acta Biomater.* **9**, 5855–5875 (2013). <https://doi.org/10.1016/j.actbio.2012.11.029>
  186. B. De Carvalho, E. Rompen, G. Lecloux, P. Schupbach, E. Dory, J.-F. Art, F. Lambert, Effect of sintering on in vivo biological performance of chemically deproteinized bovine hydroxyapatite. *Materials (Basel)*. **12**, 3946 (2019). <https://doi.org/10.3390/ma12233946>
  187. A. Watanabe, M. Sakane, T. Funayama, M. Iwasashi, A. Kanamori, N. Ochiai, Novel unidirectional porous hydroxyapatite used as a bone substitute for tibial wedge osteotomy in Canines, 14 (n.d.) 4.
  188. Z. Huang, K. Zhou, D. Zhang, Porous hydroxyapatite scaffolds with unidirectional macrochannels prepared via ice/fiber-templated method. *Mater. Manuf. Processes* **29**, 27–31 (2014). <https://doi.org/10.1080/10426914.2013.840909>
  189. F.Y. Su, J.R. Mok, J. McKittrick, Radial-concentric freeze casting inspired by porcupine fish spines. *Ceramics*. **2**, 161–179 (2019). <https://doi.org/10.3390/ceramics2010015>
  190. Y. Tang, Q. Miao, S. Qiu, K. Zhao, L. Hu, Novel freeze-casting fabrication of aligned lamellar porous alumina with a centrosymmetric structure. *J. Eur. Ceram. Soc.* **34**, 4077–4082 (2014). <https://doi.org/10.1016/j.jeurceramsoc.2014.05.040>
  191. T. Zheng, J. Li, L. Wang, Z. Wang, J. Wang, Implementing continuous freeze-casting by separated control of thermal gradient and solidification rate. *Int. J. Heat Mass Transf.* **133**, 986–993 (2019). <https://doi.org/10.1016/j.ijheatmasstransfer.2019.01.014>
  192. H. Bai, D. Wang, B. Delattre, W. Gao, J. De Coninck, S. Li, A.P. Tomsia, Biomimetic gradient scaffold from ice-templating for self-seeding of cells with capillary effect. *Acta Biomater.* **20**, 113–119 (2015). <https://doi.org/10.1016/j.actbio.2015.04.007>
  193. J. Seuba, J. Leloup, S. Richaud, S. Deville, C. Guizard, A.J. Stevenson, Fabrication of ice-templated tubes by rotational freezing: microstructure, strength, and permeability. *J. Eur. Ceram. Soc.* **37**, 2423–2429 (2017). <https://doi.org/10.1016/j.jeurceramsoc.2017.01.014>
  194. C.B. Tanaka, M. Mroz, S.E. Naleway, J.J. Kruzic, Anisotropic strength and fracture resistance of epoxy-ceramic composite materials produced by ultrasound freeze-casting. *Ceram. Int.* **48**, 4904–4910 (2022). <https://doi.org/10.1016/j.ceramint.2021.11.027>
  195. M.M. Porter, M. Yeh, J. Strawson, T. Goehring, S. Lujan, P. Siripasopstorn, M.A. Meyers, J. McKittrick, Magnetic freeze casting inspired by nature. *Mater. Sci. Eng. A* **556**, 741–750 (2012). <https://doi.org/10.1016/j.msea.2012.07.058>
  196. X. Song, H. Tetik, T. Jirakittsonthon, P. Parandoush, G. Yang, D. Lee, S. Ryu, S. Lei, M.L. Weiss, D. Lin, Biomimetic 3D printing of hierarchical and interconnected porous hydroxyapatite structures with high mechanical strength for bone cell culture. *Adv. Eng. Mater.* **21**, 1800678 (2019). <https://doi.org/10.1002/adem.201800678>
  197. G. Yang, H. Tetik, J.N. Weker, X. Xiao, S. Lei, D. Lin, In situ imaging of three dimensional freeze printing process using rapid X-ray synchrotron radiography. *Rev. Sci. Instrum.* (2022). <https://doi.org/10.1063/5.0077141>
  198. T. Li, D. Zhai, B. Ma, J. Xue, P. Zhao, J. Chang, M. Gelinsky, C. Wu, 3D printing of hot dog-like biomaterials with hierarchical architecture and distinct bioactivity. *Adv. Sci.* **6**, 1901146 (2019). <https://doi.org/10.1002/advs.201901146>
  199. J.-B. Lee, W.-Y. Maeng, Y.-H. Koh, H.-E. Kim, Novel additive manufacturing of photocurable ceramic slurry containing

- freezing vehicle as porogen for hierarchical porous structure. *Ceram. Int.* **45**, 21321–21327 (2019). <https://doi.org/10.1016/j.ceramint.2019.07.116>
200. G. Zhang, H. Chen, S. Yang, Y. Guo, N. Li, H. Zhou, Y. Cao, Frozen slurry-based laminated object manufacturing to fabricate porous ceramic with oriented lamellar structure. *J. Eur. Ceram. Soc.* **38**, 4014–4019 (2018). <https://doi.org/10.1016/j.jeurceramsoc.2018.04.032>
201. P. Parandoush, H. Fan, X. Song, D. Lin, Laser surface engineering of hierarchy hydroxyapatite aerogel for bone tissue engineering. *J. Micro Nano-Manuf.* (2018). <https://doi.org/10.1115/1.4038669>

Springer Nature or its licensor holds exclusive rights to this article under a publishing agreement with the author(s) or other rightsholder(s); author self-archiving of the accepted manuscript version of this article is solely governed by the terms of such publishing agreement and applicable law.